

Conducting Polymers as Anode Buffer Materials in Organic and Perovskite Optoelectronics

Soyeong Ahn, Su-Hun Jeong, Tae-Hee Han, and Tae-Woo Lee*

This review focuses on the importance and the key functions of anode interfacial layers based on conducting polymers in organic and organic–inorganic hybrid perovskite optoelectronics. Insertion of a buffer layer between electrode and semiconducting layers is the most common and effective way to control interfacial properties and eventually improve device characteristics, such as luminous efficiency in light-emitting diodes and power conversion efficiency in solar cells. Conducting polymers are considered as one of the most promising materials for future organic and organic–inorganic hybrid electronics because of advantages such as a simple film-forming process and ease of tailoring electrical and physical properties; as a result, using these polymers is compatible with the production of large-area, low-cost, and solution-processed flexible optoelectronic devices. This review introduces the limitations of anode buffer layers based on conducting polymers and then we will provide recent research trends of material engineering to overcome these problems.

anode (Figure 2). In this review, we focused on application of conducting polymers as an anode buffer layer of organic and organic–inorganic hybrid optoelectronic devices, including OLEDs, OSCs, PeLEDs and PeSCs. Anode buffer layers have a crucial influence on efficiency and stability of organic and hybrid optoelectronic devices. The interfaces between electrodes and semiconducting layer strongly affect the operation of optoelectronic devices by manipulating charge carrier injection or extraction, and transport.^[47–50] Also, they reduce the surface roughness of underlying anode layers and prevent local thinning which causes non-uniform current flows in devices.^[51–53]

Organic small-molecules are commonly used as hole injection or hole transporting layers in optoelectronics devices.^[54–61]

However, the standard fabrication of thin organic small-molecule films by vacuum thermal evaporation is expensive. Solution process to fabricate organic small molecule buffer layers has been tried, but it cannot be guaranteed to produce a stable film if it is based on organic small-molecules have low glass transition temperature causing the facile crystallization of the molecules without appropriate functionalization.^[62–69] Transition metal oxides are also efficient anode buffer layers.^[70–72] Although they have efficient charge injection and extraction capabilities and high stability, their inherent brittleness, difficulty in smooth film formation by solution process and requirement for high-temperature annealing are critical impediments to practical flexible device applications.^[70,72–74] Compared to these anode buffer layer materials, conducting polymers may be more suitable because they can be fabricated using solution process at a low-cost.

The most widely-used and commercially available conducting polymer is poly(3,4-ethylene dioxythiophene) doped with polystyrene sulfonic acid (PEDOT:PSS). It is solution-processable,^[5,75–81] highly transparent,^[82–86] and mechanically flexible,^[81,87–89] so it has been widely used as an anode buffer layer in organic and hybrid optoelectronic devices. However, it is hygroscopic and acidic, so it can degrade device efficiency and stability.^[4,90–93] Also, PEDOT can be de-doped because PEDOT and PSS chains are just ionically bound without covalent bonds, which can be one of reasons why PEDOT:PSS can be unstable in solution and film states. PEDOT:PSS also has insufficient work function (WF) (5.0–5.2 eV for Clevis™ P VP AI 4083)^[3,94,95] to make ohmic contact to overlying organic and hybrid materials and quenching property for excitons formed

1. Introduction

Conducting polymers feature an extended π -electron system in their main backbone. They have the electrical properties of both metals and semiconductors, while retaining the advantages of polymers such as low cost, light weight, flexibility, and simple processing, have attracted considerable attention in organic and organic–inorganic hybrid electronics. They are promising materials for use in a wide range of applications including organic light-emitting diodes (OLEDs),^[1–9] organic solar cells (OSCs),^[9–15] organic transistors,^[16–22] and photodetectors^[23–28] (Figure 1). Recently, conducting polymers have become widely used in optoelectronics on organic–inorganic hybrid perovskite (OIHP); e.g., perovskite light-emitting diodes (PeLEDs)^[29–36] and perovskite solar cells (PeSCs).^[37–46]

In optoelectronic devices including LEDs and SCs, the conducting polymers are mostly used as an anode buffer layer on

S. Ahn, S.-H. Jeong, Dr. T.-H. Han
Department of Materials Science and Engineering
Pohang University of Science and Technology
(POSTECH)

77 Cheongam-Ro, Nam-Gu, Pohang
Gyeongbuk 790-784, Republic of Korea

Prof. T.-W. Lee

Department of Materials Science and Engineering
Seoul National University

1 Gwanak-ro, Gwanak-gu, Seoul 08826, Republic of Korea
E-mail: twlees@snu.ac.kr; taewlees@gmail.com



DOI: 10.1002/adom.201600512

in adjacent emitting layers^[5,8,30,96–99]; these demerits should be solved to improve the device efficiencies and stability when PEDOT:PSS is used as an anode buffer layer.

The hygroscopic and acidic nature of PEDOT:PSS come from PSS, especially, its sulfonic acid moiety. Use of self-doped conducting polymers as a new concept of conducting polymers, in which dopant ions are covalently bound to conducting polymer chains, decreases the instability of PEDOT:PSS.^[9,39,100–102] The low WF and exciton quenching of PEDOT:PSS are also related to the doping system and resultant surface composition of its film. Therefore, material engineering should be considered as an essential steps to solve the drawbacks of PEDOT:PSS.

In this review, several material engineering approaches to overcome the limitations of conventional conducting polymer-based anode buffer layer will be discussed. In Section 1, the conduction mechanism of conducting polymers will be introduced, and the historical background of conducting polymers as anode buffer layers in organic and hybrid optoelectronic devices will be presented. We will explain why anode buffer layers are required in organic and hybrid optoelectronic devices, and discuss the drawbacks of conventional anode buffer layers. Section 2 reviews the attempts to overcome the limitations of conducting polymers as anode buffer layers. Sections 3 and 4 will provide the importance of engineering of conducting polymers for the anode buffer layer in organic and hybrid optoelectronic devices.

1.1. Conduction Mechanism of Conducting Polymers

1.1.1. Conduction Mechanism

For polymers to be electrically conductive, they must have π -conjugated polymer chains; i.e., continuously overlapping π -orbitals along their main backbone which allow delocalization of charge carriers.^[103] However, π -conjugated polymers are not electrically conductive without any further chemical treatment.^[104] For polymers to be conductive, the charge carriers should be able to move freely through their structure, as in metal. Therefore, doping agents that can remove electrons (p-doping) or add electrons (n-doping) for delocalizing π -orbitals are introduced to the polymer so that charge carriers in the orbital can move along the polymer chain.^[103,105–109]

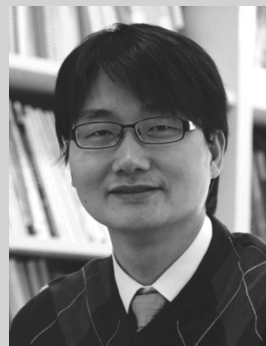
The conduction mechanism of conjugated polymers can be explained based on a quasi one-dimensional system, which describes the mechanism in terms of solitons, polarons, bipolarons and the energy band model.^[107] Conjugated polymers can be categorized according to whether the ground state of the polymer is degenerate or non-degenerate (Figure 3a). The first conducting polymer, polyacetylene (PA), was a *trans* isomer composed of only C and H, with a structure of alternating C–C single and C=C double bonds; it is the prototype degenerate-ground-state polymer.^[109] Two chain configurations of *trans*-PA have the same energy in the ground state and the interchange between the single and double bonds can happen without any change in energy.^[110] When the two ground states meet, a structural defect in a form of a free radical is produced; the resultant defect is a neutral soliton (S^0) in the middle of the band gap (mid-gap) (Figure 3b).^[110] Energy band theory states



Soyeong Ahn is currently a Ph.D. candidate in Materials Science and Engineering at Pohang University of Science and Technology (POSTECH), Korea. She received her M.S. and B.S. degrees in Chemical Engineering from Kyung Hee University in February 2015. Her current research focuses on conducting polymers for flexible organic and organic–inorganic hybrid optoelectronic devices.



Su-Hun Jeong received his B.S. in Materials Science and Engineering in 2012 from Pohang University of Science and Technology (POSTECH). He is a graduate student in POSTECH since 2012. His current research work is focused on polymeric electrodes for flexible organic optoelectronic devices.



Tae-Woo Lee is an associate professor in Materials Science and Engineering at Seoul National University, Korea. He received his Ph.D. in Chemical Engineering from KAIST, Korea in 2002. He joined Bell Laboratories, USA as a postdoctoral researcher and worked in Samsung Advanced Institute of Technology as a member of research staff (2003–2008). He was an associate professor in Materials Science and Engineering at Pohang University of Science and Technology (POSTECH), Korea until Aug, 2016. His research focuses on printed electronics based on organic and organic-inorganic hybrid materials for flexible displays, solid-state lightings, and solar-energy-conversion devices.

that the alternation of single bonds with double bonds in the π -conjugated polymers is a result of Peierls distortion, which causes a band gap at the Fermi level of the polymer.^[110,111] For this reason, these polymers exhibit semiconducting behaviors instead of metallic behaviors.^[110,112]

However, for conjugated polymers to be conductive at room temperature (RT), charge carriers in the polymer backbone must be able to flow through the conduction band at RT. The



Figure 1. Applications of conducting polymers to organic and organic–inorganic hybrid perovskite electronics such as OSCs, upper image: Reproduced with permission.^[10] Copyright 2014, WILEY-VCH. lower image: Reproduced with permission.^[9] Copyright 2011, WILEY-VCH, OLEDs, Reproduced with permission.^[4] Copyright 2007, WILEY-VCH, organic transistors, Reproduced with permission.^[22] Copyright 2013, Nature Publishing Group, photo detector, PeLEDs, upper image: Reproduced with permission.^[30] Copyright 2014, WILEY-VCH, lower image: Reproduced with permission.^[31] Copyright 2015, American Association for the Advancement of Science, PePVs, right image: Reproduced with permission.^[37] Copyright 2014, WILEY-VCH.

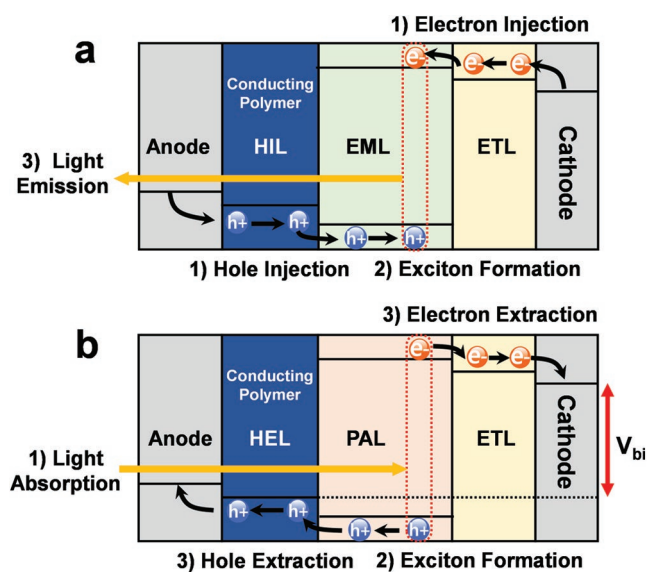


Figure 2. Schematic band diagram of a) light-emitting diodes with a hole injection anode buffer layer and b) solar cells with a hole extraction buffer layer.

neutral soliton (S^0) has spin $\frac{1}{2}$. Positive (S^+) and negative solitons (S^-) can also be generated by a doping process (removing or adding an electron to the system); charged solitons have no spin.^[107,110] Increase in the number of removed or added electrons (i.e., increase in the doping level) increases the number of electronic states of charged solitons that interact with each other and overlap. This overlap produces a soliton band in the middle of the gap between conduction and valence bands^[113] (Figure 3c); as a result, degenerate polymers can have electrical conductivity.

However, most π -conjugated polymers have a non-degenerate ground state; instead, they are composed of benzoid and quinoid structures.^[103,112,113] Their structures are energetically inequivalent (Figure 3a): the polymer with the benzoid structure (the neutral form) has lower energy than that with the quinoid structure (the oxidized form).^[110] Therefore, the soliton is driven to the end of the polymer chain; during this motion, the soliton changes the quinoid rings to benzoid rings. To prevent this transition, bound double-defects (a neutral combined with a charged soliton) can be created by removing electrons from or adding electrons to the system in the same manner used for the degenerate polymer.^[114] Such double-defects are called as polarons.

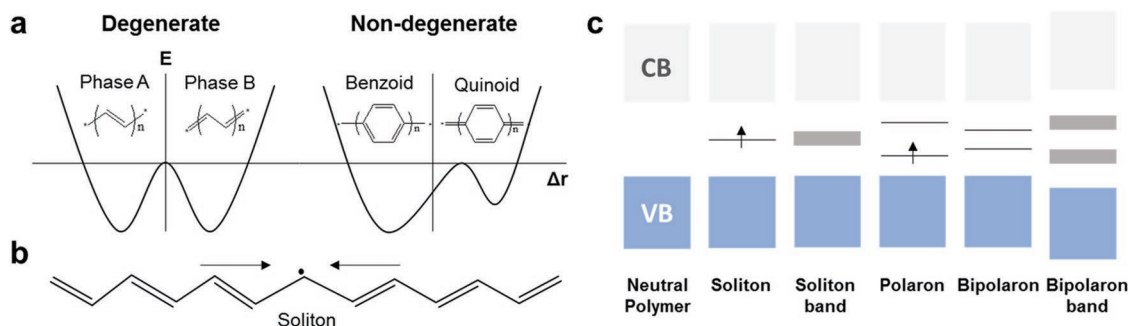


Figure 3. a) Schematic representation of the potential energy change depending on the deformation coordinate of conjugated polymer with degenerate ground state (*trans*-polyacetylene (*trans*-PA)) and non-degenerate ground state (poly(*p*-phenylene) (PPP)). b) Formation of soliton in *trans*-polyacetylene. c) Band theory in conducting polymers. CB: Conduction band, VB: Valence band.

In chemistry, the positive polaron (a neutral soliton and a positive charge) and the negative polaron (a neutral soliton and a negative charge) are called the radical cation and radical anion, respectively.^[115] The two solitons travel in opposite directions to minimize the high-energy quinoid part of the chain but the solitons in the non-degenerate polymers cannot move freely because the total energy increases as two solitons depart from each other. Consequently, the solitons produce a confined pair with both charge $\frac{1}{2}$ and spin $\frac{1}{2}$ (polaron), which induce a localized distortion towards the higher-energy quinoid form in the polymer chain.^[114] At this time, the mid-gap energy states of the solitons hybridize and form new localized electronic states in the band gap (Figure 3c).

Further oxidation or reduction induces coupling of two polarons to yield bipolarons, which have no spin and are doubly-charged. The bipolarons also have new electronic states but they are locally shifted away from the electronic states of the polarons because the bipolarons are stabilized by the energy gained from the distortion overlapping. In a similar way, bipolarons form a band at high doping concentration and the band eventually merges with the conduction and valence bands to produce metallic conductivity.^[108] The charge transport mechanism of the conducting polymer is reported to be primarily influenced by intrachain band diffusion, interchain hopping of polarons, bipolarons, or both.^[107]

1.1.2. Concept of Doping in Conducting Polymers

After the discovery of electrically-conductive polyacetylene (PA),^[109] various conducting polymers such as polypyrrole (PPy),^[116] polyaniline (PANI),^[117,118] polythiophene (PTh),^[115] poly(phenylene vinylene) (PPV)^[112,115] and PEDOT^[119] have been reported (Figure 4). These conducting polymers are achieved by electrical doping. Several types of electrical doping (e.g., chemical, electrochemical, photo, interfacial) can be used depending on the purpose and applicability.^[120–126] Chemical doping is the classical and the most commonly-used doping method^[127–131]; it can be achieved by exposing polymer films to dopants of vapor or liquid. Usually, oxidizing (p-type) dopants have electron-attracting property, whereas reducing (n-type) dopants have electron-donating property. The doping process is conducted during synthesis. Most conducting polymers are synthesized by oxidative polymerization which uses an oxidizing

agent that has strong oxidizing power, or by applying higher voltage than the oxidation potential of the monomer.^[104,132–138] For example, PEDOT:PSS can be synthesized by using ferric chloride or iron(III) *p*-toluenesulfonic acid (tosylate) as an oxidizing agent in the presence of its monomer, 3,4-ethylenedioxythiophene (EDOT) and the dopant, PSS.^[139] The polymeric dopant surrounds the conducting polymer chains and makes them be dispersed in the solvents, and therefore acts as both charge-compensating counter-ion and soluble template for the conducting polymer. Therefore, the types and amount of dopants are key factors to determine solubility of the conducting polymer along with electrical conductivity.^[127,140,141] When a π -conjugated polymer is doped with a strong basic center, proton doping is preferred.^[118] In contrast to redox doping, proton doping does not change the number of electrons in the polymer chain. PANI is a typical example of the conducting polymer prepared by proton doping.^[117,118]

The dopants can be classified into three categories: neutral dopants (e.g., I_2 , Br_2 , AsF_5 , Na, K), ionic dopants (e.g., LiClO_4 , FeClO_4 , $\text{CF}_3\text{SO}_3\text{Na}$) and miscellaneous organic and polymeric acid dopants.^[142,143] Organic and polymeric acids are frequently used to increase doping stability. However, polymers doped with small molecules often have negligible solubility, and therefore are not easily processable.^[140] The processable conducting polymers are generally prepared by aqueous colloidal dispersion in the presence of water-soluble anion surfactants (acid dopants) and form ionic bonds with the acid dopants (Figure 4).^[75,142,144] Frequently used dopants include camphor sulfonic acid (CSA),^[140,145–147] *p*-toluene sulfonic acid (*p*-TSA),^[139,140,148] dodecylbenzene sulfonic acid (DBSA),^[127,128,140,147] polyvinyl sulfonic acid (PVSA),^[148,149] poly(2-acrylamido-2-methyl-1-propane sulfonic acid) (PAMPS)^[150,151] and polystyrene sulfonic acid (PSS).^[75,130,145] Fluorosurfactant such as perfluorooctane sulfonic acid (PFOS)^[152,153] and poly(perfluoroethylene perfluoroethersulfonic acid) (PFFSA)^[154] can also be used as acid dopants.

The morphological, electrical, and optical properties of the conducting polymer vary with the dopant used and the doping level.^[110,113,118] Due to steric hindrance, the size of the dopant ion affects the electrical conductivity of the polymer.^[150,151] However, the behavior of a doping system is complex, so this relationship between dopant size and the doping level is not straightforward.^[140] The doping level represents the extent of oxidation or reduction and thus primarily determines the

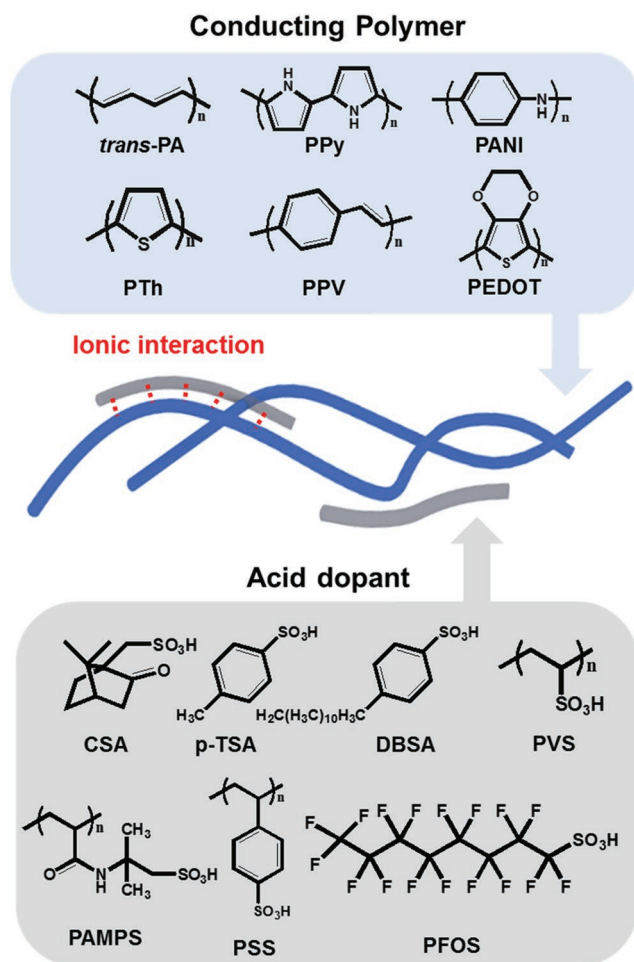


Figure 4. Molecular structures of conducting polymers and acid dopants.

electrical conductivity of the conducting polymer.^[117] The electrical conductivity increases as the doping ratio increases (Figure 5).^[146,155] The doping level is generally controlled by the dopant concentration of the conducting polymer. Doped PANI:CSA film shows an increased WF and electrical conductivity due to the Fermi level shifts toward the valence band upon doping.^[146] The WF of PANI:CSA film was increased from 4.42 eV to 4.78 eV and its electrical conductivity was increased from 2 S cm⁻¹ to 217 S cm⁻¹ by adjusting the PANI to dopant molar ratio from 1:0.25 to 1:1.^[146]

1.2. Conducting Polymer-Based Anode Buffer Layer in Organic and OIHP Optoelectronics

1.2.1. Historical Background of Conducting Polymers for Anode Buffer Layer

In OLEDs, PPV was the first conjugated polymer to be used as an emitting layer.^[156] The first, polymer light-emitting diodes (PLEDs) consisted of a transparent anode (generally composed of indium-tin-oxide (ITO)), an electroluminescent conjugated polymer and a metal cathode without any buffer layers between the electrodes and the emitting layer. Hetero-structure OLEDs

that use PPV as hole injection layer were proposed to achieve efficient charge injection by improving energy-level alignment.^[157,158] The UNIAX group suggested a PANI:CSA film as an anode buffer layer for a PLED that uses poly(2-methoxy-5-(2-ethylhexyloxy)-1,4-phenylenevinylene) (MEH-PPV) as an emitter.^[159] The energy barrier between the anode and the MEH-PPV was reduced from 0.2 eV to ≈0.1 eV by inserting a PANI:CSA film between them.^[159] The operating voltage of the resulting device was reduced by 30–50% and the quantum efficiency was increased by 30–40% compared with those of the device that lacked the anode buffer layer.^[159] PPy-DBSA film was also suggested as an anode buffer layer for PLEDs that use a MEH-PPV emitting layer, but because of the high energy barrier of 0.23 eV between the PPy-DBSA and the MEH-PPV, devices with this layer had a lower quantum efficiency (0.5%) than did device that used the PANI:CSA film as an anode buffer layer (1.5%).^[147]

In a similar approach, device efficiency was improved significantly by coating the ITO with a PANI film, doped with polyacid.^[160] The PLEDs using MEH-PPV as an emitter and the PANI film as an anode buffer layer exhibited a higher efficiency of 1.4 lm W⁻¹ than PLEDs without the anode buffer layer (0.8 lm W⁻¹) at the same voltage (5 V).^[160] PANI:CSA precipitates in water and therefore must be prepared as an organic solvent solution, but the polyacid-doped PANI film can be prepared in a water-dispersed form (PanAquasTM).^[160] The water-dispersed polyacid-doped PANI has better processability and higher doping stability than the organic-solvent-dispersed small molecule acid-doped PANI.^[141,161] A major increase in device efficiency was achieved by introducing PEDOT:PSS as an anode buffer layer, mainly because PEDOT:PSS has a relatively higher WF (5.0–5.2 eV for ClevisTM P VP AI 4083)^[3,94,95] than do previously-reported conducting polymers (e.g., WF of PANI:CSA ≈ 4.8 eV).^[146,147,162] The PEDOT:PSS has been a commercial success for anode buffer layer in organic optoelectronic devices. The commercially available PEDOT:PSS solutions have several types according to the ratio of PEDOT to PSS.^[3,163] Electrical conductivity and work function of PEDOT:PSS can be controlled by varying ratio of PEDOT to PSS (10⁻³–10 S cm⁻¹, 4.8–5.2 eV). Recently, PEDOT:PSS has been most widely used as the anode buffer layers in PeLEDs^[29,30,32–36] and PeSCs.^[37–46]

1.2.2. Requirements of Anode Buffer Layer for Optoelectronic Devices

The efficiency of optoelectronic devices is strongly dependent on the properties of the interfaces between stacked layers;^[2,164–166] therefore the efficiency of the devices can be advanced by controlling these properties. The simplest and most effective way to modify the interface states is to insert buffer layers (also called interfacial layers or interlayers) between the stacked layers. Properties of buffer layers strongly influence on device efficiency and device lifetime.

The primary function of an anode buffer layer is to facilitate hole injection into or extraction from the semiconducting layer. For good hole injection or extraction, an anode must make Ohmic contact with an overlying active semiconducting layer to reduce injection barrier in LEDs or potential loss in

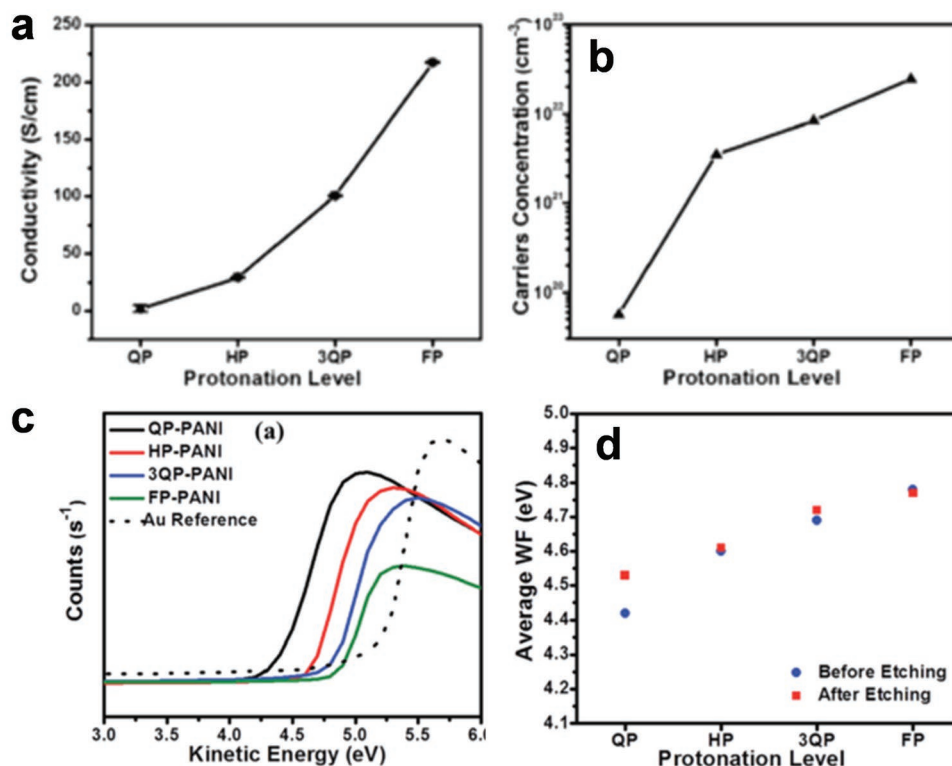


Figure 5. Effects of doping level of conducting polymer. Effect of CSA protonation levels on a) electrical conductivity of PANI, and b) carrier concentration of PANI:CSA versus protonation levels. c) Kinetic energy cut-off of XPS measured on PANI:CSA films. d) Surface work function of PANI before and after etching depending on protonation levels. a–d) Reproduced with permission.^[146] Copyright 2015, Royal Society of Chemistry.

SCs. However, the low WF of ITO ($\approx 4.7\text{--}4.9\text{ eV}$)^[3,167–170] is insufficient to form Ohmic contact with the highest occupied molecular orbital (HOMO) energy level of $\approx 5.4\text{--}5.9\text{ eV}$ ^[56,171,172] for organic emitters and $\approx 5.15\text{--}5.5\text{ eV}$ ^[173–176] for organic photoactive materials (Figure 6). Also, the deep valence band maximum (VBM) of OIHP materials ($\approx 5.4\text{--}6.0\text{ eV}$) imposes high energy barrier with ITO anodes.^[30,31,37,38,40] Therefore, to form Ohmic contact with the semiconducting layers, anode buffer layers with high WF are required; i.e., energy-level alignment achieved by using anode buffer layers with high WF reduces the energy barrier and increases built-in potential, and thereby

facilitates hole carrier injection in LEDs and increases open-circuit voltage in SCs.^[3,4,6,30,38]

At the same time, the materials for anode buffer layer should have high mechanical, chemical and electrical stability. An ideal anode buffer material must not affect the electrode and semiconducting layer and also not be affected by the overlying layers to avoid degradation of device efficiency and stability.

Another important function of the anode buffer layer is to smooth the surface of electrodes. Transparent conducting oxide (TCO) materials that are generally used as transparent electrodes in optoelectronics normally have rough surfaces,

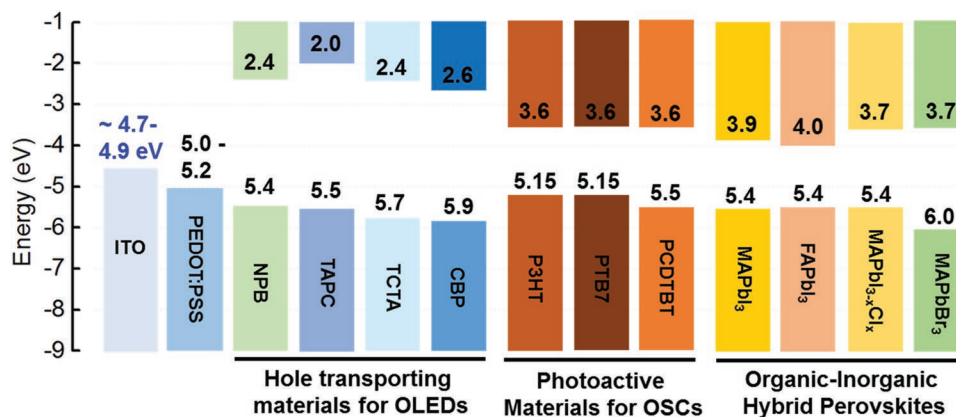


Figure 6. Schematic energy bands of organic and OIHP semiconducting materials for OLEDs, OSCs, PeLEDs and PeSCs.

which can induce leakage current and internal short-circuit due to the uneven thickness of overlying layer; the consequences include degraded device efficiency and stability.^[51–53] To avoid this happening, the anode buffer layer should have a good film-forming property so that it forms uniform film with low surface roughness.

In a device configuration in which light is transmitted through the anode, the anode buffer layer must have high transmittance over a wide range of wavelengths, so that light entering the device or generated by the semiconducting layer not to be interrupted.

To summarize, the basic requirements of anode buffer materials for optoelectronic devices are (1) high WF enough to inject holes into or to minimize the potential loss at the interface of hole extraction from the semiconducting layer, (2) high mechanical, chemical and electrical stability, (3) good film-forming property to smooth the surface of the electrode and (4) high transmittance in a device configuration that includes a transparent anode as a light input and output window.

1.2.3. Limitations of the Conventional Anode Buffer Materials

Organic small-molecular anode buffer layers have been widely used in multilayered OLEDs to inject hole carriers from the anode into organic layers. However, the standard method to fabricate organic small-molecule layers for multilayered organic devices is vacuum thermal evaporation which is expensive. Although solution-processing of organic small-molecules has been attempted to fabricate OLEDs or OPVs at a low cost,^[177–180] conventional hole injecting or transporting organic small-molecules such as N,N0-diphenyl-N,N0-bis(3-methylphenyl)-(1,10-biphenyl)-4,40-diamine (TPD), 1,4-bis(1-naphthylphenyl-amino) biphenyl (NPB), 1,1-bis((di-4-tolylamino)phenyl)cyclohexane (TAPC) have low glass transition temperature, so they may crystallize during solution processing; as a result, the film can be unstable.^[62–69] Alternative materials are necessary. Inorganic transition metal oxides such as MoO₃ and V₂O₅ have excellent charge injection or extraction properties and are very stable.^[70–72] However, their poor film-forming property results in a rough surface, which can cause leakage current and electrical shorts in thin-film devices.^[70–72,181,182] The transition metal oxide-based anode buffer layers can also be formed by using a solution process, but their precursor molecules should be thermally converted by high-temperature heating.^[74,183,184] This high-temperature process has limited the wide practical use of the transition metal oxides in organic devices, especially, flexible devices which use flexible substrates with low glass transition temperature. Furthermore, because transition metal oxides are mechanically brittle, their applications in flexible electronics are limited.^[73,185,186] A few nanometer-thick-graphene oxide (GO) sheet obtained by oxidation of graphite, has also been used as an anode buffer layer in organic optoelectronic devices.^[187–191] However, a buffer layer composed of GO cannot make a flat film surface, and reproducibility is low, so practical applications are currently limited.^[192,193]

The conducting polymer PEDOT:PSS is generally used as the anode buffer layer in organic and OIHP optoelectronic devices. The advantages of PEDOT:PSS (e.g., high transparency,

superior mechanical flexibility, solution processability) make it the most widely-used anode buffer layer. However, several disadvantages such as (1) hygroscopic property, (2) strong acidity, (3) low WF, (4) exciton quenching and (5) particle aggregation reduce the device efficiency and lifetime.

The hygroscopic property of PEDOT:PSS causes water uptake during or after film preparation. The humidity and the temperature during the polymer storage or processing have a huge effect on the polymer chain conformation and consequently its properties, and therefore degrade the reproducibility of the resulting devices.^[87,88] Also, the water absorption can form an acidic aqueous environment by the reaction $\text{H}_2\text{O} + \text{PSS}(\text{HSO}_3) \rightarrow \text{H}_2\text{O}^+ + \text{PSS}(\text{SO}_3)$; and this facilitate etching of the ITO anode which results in release of metallic In and Sn.^[90] Absorbed water molecules may also reduce the electrical conductivity of PEDOT:PSS; as a result the device degrades.^[90,194] OIHP is also degraded by water, but the mechanism is still under study.^[195–204]

The another major impediment to using PEDOT:PSS as a buffer layer in optoelectronic devices is that the PEDOT:PSS film is strongly acidic, and therefore etches transparent oxide electrodes that are widely used in optoelectronics.^[4,90–92] Metal ions such as In and Sn etched from ITO can easily diffuse into overlying layers during device fabrication and operation. Indium oxide (In₂O₃) is highly soluble in acid, and In ions can migrate into the PEDOT:PSS film.^[4,90,188,205] Diffused and migrated metal ions can form trapping sites or non-radiative exciton recombination centers in organic and hybrid optoelectronic devices.^[4,43,90,205] Charge trapping by diffused metal ions can increase operating voltage, and can degrade charge balance in devices.^[6] Exciton quenching caused by metal impurities also decreases efficiency of optoelectronic devices.^[8,90] Therefore, the acidic nature of PEDOT:PSS can degrade device efficiency and operational stability.

In OLEDs and PeLEDs, device efficiency is determined by the behavior of injected charge carriers, and the charge carrier injection is controlled by the band offset between the anode and the emitting layer. A change of a few tenths of an electron volt in the energy barrier affects the operating voltage of the device and consequently the device efficiency and lifetime.^[4,5,8,30,206] Likewise, the band offset between the anode and active layer of SCs affects the potential loss at the hole extraction interface, decreasing the open-circuit voltage (V_{oc}) of the devices.^[37,39,207,208] To achieve efficient LEDs or SCs, the anode buffer layer must form Ohmic contact with the semiconducting layer. Because most organic and OIHP semiconducting materials have deep HOMO or VBM of 5.4–6.0 eV,^[31,40,56,170–175] (Figure 6), the high energy band offset that is caused by low WF of PEDOT:PSS (5.0–5.2 eV for Clevios™ P VP Al 4083)^[3,94,95] is a serious obstacle to the use of PEDOT:PSS in LEDs and SCs.

PEDOT:PSS is a strong exciton quencher. Several studies have observed luminescence quenching at the interface between PEDOT:PSS and the organic layer when the recombination zone is adjacent to the PEDOT:PSS.^[5,8,30,96–99] Exciton quenching can be mainly caused by exciton migration (or non-radiative energy transfer) to bipolarons in oxidized (doped) PEDOT or exciton dissociation caused by large energy level offset between oxidized PEDOT and an organic emitter which is larger than exciton binding energy of emitting materials.^[8]

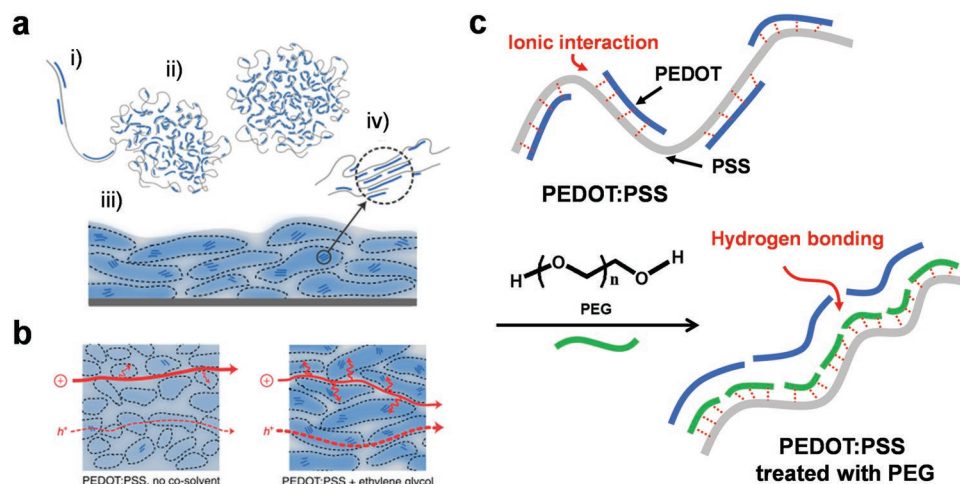


Figure 7. Conductivity enhancement mechanism of polar solvents. a) Schematic structure of PEDOT:PSS; i) commonly-described microstructure of the conducting polymer system, ii) formation of colloidal gel particles in dispersion, iii) resulting film with PEDOT:PSS-rich (blue) and PSS-rich (grey) phases, and iv) aggregates/crystallites supporting enhanced electronic transport. b) Schematics of ion and hole transport before and after adding a polar solvent, EG. a,b) Reproduced with permission.^[221] Copyright 2016, Nature Publishing Group. c) Schematic mechanism of conductivity enhancement by PEG. Reproduced with permission.^[220] Copyright 2013, Royal Society of Chemistry.

Chemical interaction between PEDOT:PSS and the semiconducting layer can induce additional exciton quenching.^[96]

Another huge disadvantage of using PEDOT:PSS as an anode buffer layer in optoelectronic devices is poor stability during storage or during device operation.^[144,209] Changes in environmental conditions during these processes can affect the net electrostatic charge on the PSS chains and thus change the electrostatic interaction between PEDOT and PSS, which result in the de-doping process of the PEDOT:PSS, so particles of PEDOT:PSS may aggregate; the result is inferior film-forming property.^[209–212]

De-doping also occurs during device operation as a result of electrochemical oxidation and reduction of PEDOT:PSS film.^[209,210] The aggregated PEDOT and PSS particles can create defects that can trap charge carriers, and thereby cause increase in the voltage required to drive charge carriers through the device.^[26,213–216] This increase in the operating voltage decreases the device lifetime.

In short, the conventional PEDOT:PSS has disadvantages such as (1) hygroscopicity, (2) strong acidity, (3) low WF, (4) exciton quenching and (5) particle aggregation that can reduce the device efficiency and lifetime. However, material engineering can tailor the properties of the conducting polymer, and thereby overcome these limitations.

The hygroscopic and acidic properties of PEDOT:PSS film that originated from the sulfonic acid groups of the PSS chains can be reduced by manipulating the PSS part in the polymer. The WF of PEDOT:PSS and the exciton quenching behavior at the film surface are influenced by the surface property of PEDOT:PSS film, and therefore modification of the surface composition can increase the WF of the conducting polymer and reduce the exciton quenching at the interface between it and the semiconducting layer. The limitations of the conventional PEDOT:PSS have led to use of different types of conducting polymers as an anode buffer layer; for example, a water-soluble self-doped conducting polymer that has high storage

stability and device operational stability can replace the conventional water-dispersible conducting polymer.^[100–102]

The next section reviews approaches to material engineering of the conventional conducting polymer.

2. Material Engineering of Conducting Polymer-Based Anode Buffer Layer

Material engineering to develop stable and efficient anode buffer layers by overcoming the demerits of the conventional conducting polymer involves changing material composition, surface composition, molecular structure of conducting polymers and also developing new conducting polymers, composites or blends.^[3,217,218]

The hygroscopic and strongly acidic properties of PEDOT:PSS are a consequence of free PSS in the polymer.^[219] Reducing the amount of free PSS in PEDOT:PSS film surface can prevent diffusion of water molecules in the air into the polymer film and thereby increase the stability of the film.^[11,220] The amount of free PSS in the film surface can be reduced by adding polar organic compounds (e.g., ethylene glycol (EG), dimethylsulfoxide (DMSO)) into PEDOT:PSS aqueous solution (Figure 7a).^[11,220,221] The addition of these polar solvents into the aqueous PEDOT:PSS solution involves phase separation between the PEDOT and the PSS chains leading to (1) reorientation of the polymers in a way that increases their interconnectivity by addition of solvents that have high-boiling temperature as plasticizers;^[12,222–224] (2) screening effect that inhibits coulomb electrostatic interaction between them;^[224,225] and (3) removal of excess PSS chains during the film-forming process.^[11,223,224] The phase separation between PEDOT and PSS chains, and the chain conformation change from a coil to a linear or extended coil caused by the addition of a polar solvent are main origins of the increase in electrical conductivity of PEDOT:PSS after addition of polar organic compounds (Figure 7b).^[226,227]

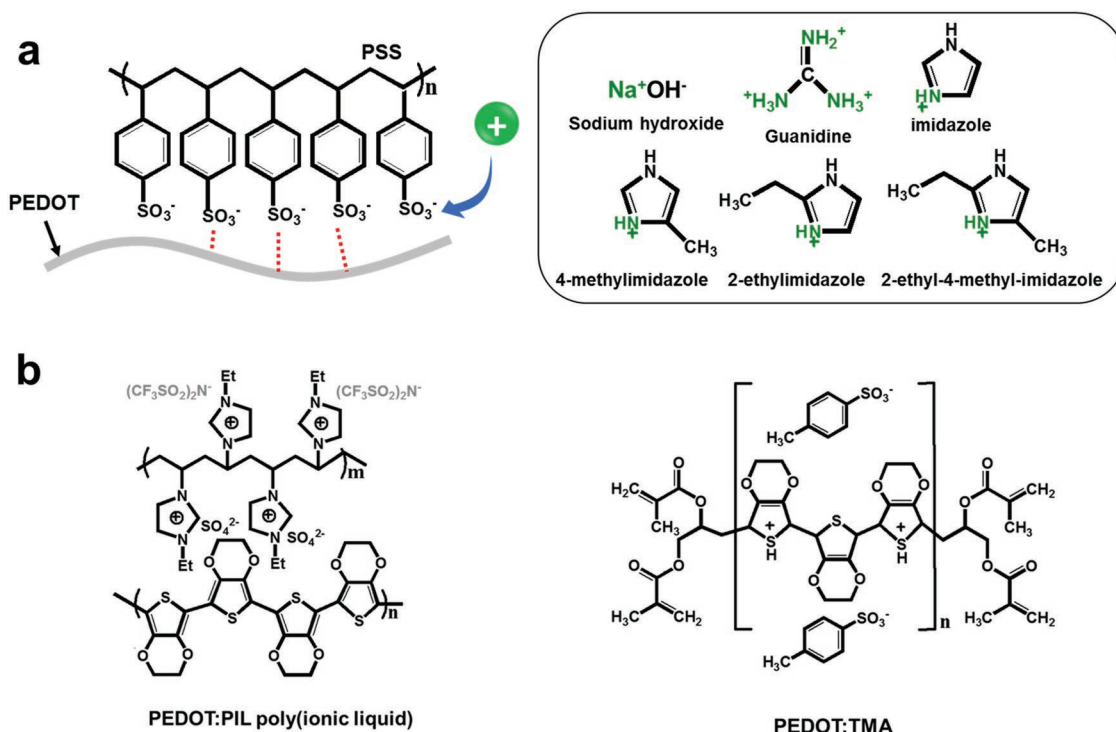


Figure 8. Material engineering to reduce hygroscopic and acidic properties of the conducting polymer. a) Additives for reducing acidity of PSS. b) Conducting polymers with reduced acidity.

The electrical conductivity of PEDOT:PSS film decreases over time due to the moisture absorption by hygroscopic PSS, but the rate can be reduced when EG or polyethylene glycol (PEG) is added (Figure 7c).^[220] When the prepared films are placed in ambient condition at RT and relative humidity >75%, untreated PEDOT:PSS film maintained only 32% of its initial conductivity after 20 days, whereas PEDOT:PSS film treated with EG maintained up to 52% and PEDOT:PSS film treated with PEG maintained 66%.^[220] This stability enhancement of PEDOT:PSS film treated with EG or PEG under humidity is attributed to hydrogen bonds formed between EG or PEG and PSS. The film treated with PEG has bigger particles than the film treated with EG. It implies that a large molecular weight PEG facilitates interconnection between PEDOT chains, leading to high electrical conductivity and stability of PEDOT:PSS film.

Post treatment of PEDOT:PSS film with polar solvent DMSO can also cause PSS depletion at the film surface.^[11] Compared to pristine film, PEDOT:PSS films doped with 6 vol.% EG had higher electrical conductivity and slower decrease in electrical conductivity over time. The rate of decrease in electrical conductivity over time was further reduced when the solvent post-treatment time was increased.^[11] The surface ratio of PSS to PEDOT was 1.37:1 in the film that had been treated with solvent and 2.15:1 in the film that had not been treated.^[11] The results indicate that PSS depletion at the surface increases the stability of PEDOT:PSS film under humid conditions.

The hygroscopic and strongly acidic properties also can be reduced by modifying the sulfonic acid groups in the PSS chains which do not form an ionic bond with the PEDOT, or

by replacing the PSS dopant with other dopants that are less hygroscopic and less acidic than PSS.

To reduce the acidity of PEDOT:PSS, the pH of PEDOT:PSS can be controlled by chemical treatment with various additives. Examples of the additives are presented in Figure 8a. Addition of a small amount of the strong base sodium hydroxide (NaOH) to PEDOT:PSS solution neutralized PEDOT:PSS by altering PSS-H to PSS-Na.^[210,228,229] The pH of PEDOT:PSS solution is controlled by the amount of NaOH in PEDOT:PSS solution and can be increased to pH >10, but a large amount of NaOH is required to make neutral solution (pH ≈7) because of the slow pH relaxation effect.^[210,230] Pristine PEDOT:PSS intrinsically includes PSS-Na as well as PSS-H, and the acidic PSS-H has greater potential to generate carriers than does the neutralized PSS-Na: and therefore the alteration of PSS-H into PSS-Na affects the carrier concentration of PEDOT:PSS film.^[228] Addition of only 0.2 molar ratio of NaOH can remove more than 20% of the sulfonic acid groups and increase the device lifetime, but further addition of NaOH leads to decreased electrical conductivity and lowered WF, possibly as a result of a dedoping process and a reduced interconnection between PEDOT chains caused by the excess NaOH molecules remained even after neutralizing sulfonic acid groups in free PSS.^[228]

Guanidine has also been used to develop pH-neutral PEDOT:PSS.^[92,231,232] Guanidine is a strong base: it produces OH⁻ in water by forming NH₃⁺ and NH₂⁺, then the OH⁻ neutralizes H⁺ (Figure 8a).^[92] The pH-neutral PEDOT:PSS obtained in this way shows high storage and operational stability.^[232] Use of NaOH and guanidine successfully neutralized acidic PEDOT:PSS, but a loss of electrical conductivity was inevitable.

Imidazole and its derivatives, which are weak bases, have been suggested as alternative neutralizing agents that can enhance the stability of PEDOT:PSS with minimal loss of electrical conductivity.^[233] Although the electrical conductivity of PEDOT:PSS film showed gradual decrease when pH increased as the film was treated with imidazole or its derivatives, the reduction was not significant; this method achieved the highest electrical conductivity (685.2 S cm^{-1}) among pH-neutral PEDOT:PSS films reported to date.^[231,233]

A non-acidic and non-hygroscopic conducting polymer, PEDOT doped with poly(ionic liquid) (PEDOT:PIL), dispersed in organic solvent has been reported (Figure 8b).^[234] The PEDOT:PIL was prepared by PIL-mediated polymerization. Imidazolium-based PILs with trifluoromethanesulfonyl imide ($(\text{CF}_3\text{SO}_2)_2\text{N}^-$ or TF_2N^-) were used as a soluble template for PEDOT.^[234] Compared to PEDOT:PSS, PEDOT:PIL is stable and less sensitive to water because it does not have acidic moieties unlike conventional conducting polymers and it is dispersed in organic solvents. Lifetime of OLED device with a PEDOT:PIL anode buffer layer was about five times longer than that with PEDOT:PSS.^[234] This finding indicates that development of organic solvent-soluble (organo-soluble) conducting polymers can be an effective strategy to avoid water absorption during or after film preparation. Organo-soluble and non-corrosive conducting polymer, PEDOT-tetramethacrylate (TMA), can be an alternative to the hygroscopic and acidic PEDOT:PSS.^[235] The PEDOT-TMA has a modified PEDOT structure in which both ends of the polymer are capped, so the chain length is limited. The short chain of the PEDOT-TMA makes it soluble in organic solvents.

Other recent research to reduce the detrimental effects of the hygroscopic and acidic properties of PEDOT:PSS has combined PEDOT:PSS with stable inorganic materials (e.g., MoO_3 , GO).^[45,236–242] When a MoO_3 /PEDOT:PSS bilayer is used as an anode modification layer, the MoO_3 layer prevents the interfacial degradation caused by the acidic PEDOT:PSS layer.^[236] PEDOT:PSS: MoO_3 hybrid system was also proposed to reduce the hygroscopic property of PEDOT:PSS along with its acidity, which also reduces the device lifetime.^[237,238] OSCs that use PEDOT:PSS: MoO_3 composite film as an anode buffer layer showed greatly extended device lifetime compared to OSCs that use only PEDOT:PSS film as a buffer layer. Ten days after fabrication, the power conversion efficiency (PCE) of the PEDOT:PSS: MoO_3 -based device only fell by 20%, whereas PCE of PEDOT:PSS-based device fell to zero.^[237] The PEDOT:PSS: MoO_3 film may inhibit diffusion of moisture from the buffer layer to the cathode.

GO has been used in approaches similar to that used with MoO_3 . A GO/PEDOT:PSS bilayer was also introduced as an anode buffer layer in planar heterojunction $\text{CH}_3\text{NH}_3\text{PbI}_3$ -based PeSCs.^[45] Use of the GO layer between the ITO anode and PEDOT:PSS layer prevented etching of ITO by the acidic PEDOT:PSS, and therefore extended the lifetime of the device.^[45]

The low WF of the conducting polymer remains one of major challenges. Although doping of the conducting polymer can increase its WF, it is not enough to facilitate hole injection into the overlying semiconducting layers.^[146] Tuning the WF requires changing the surface composition of the conducting

polymer. The surface composition of PEDOT:PSS can be modified by controlling thermal annealing temperature and time, changing the solvent, changing the chain conformation of the polymer, or by controlling the molecular weight and surface energy of polymeric acid additives to PEDOT:PSS solution.^[3–5,194,218]

The chain conformation can be modified by solvent treatment.^[226,227] A representative strategy is the polar solvent additive method.^[11,12,222–224] Polar solvent vapor annealing (PSVA) was also proposed to modify the polymer chain conformation and thereby the surface composition of the film (Figure 9a).^[218] Contrary to the conventional solvent additive method, the PSVA approach increased both the conductivity (up to 1057 S cm^{-1}) and the WF (up to 5.35 eV) of PEDOT:PSS film (Figure 9b,c).^[218] These changes were attributed to spontaneous vertical phase separation between PEDOT and excess PSS chains that were induced by the polar solvent vapor during annealing process.

Ultraviolet (UV) or UV-ozone plasma exposure of PEDOT:PSS film is another approach to increase the WF of PEDOT:PSS anode buffer layer. The UV or UV-ozone treatment changes the chain conformation of PEDOT:PSS from a coil to a linear or extended coil and decreases the number of charge-trapping-related defects at the surface, thereby increasing both the electrical conductivity and the WF (ΔWF : $0.2 \approx 0.25 \text{ eV}$).^[7,243]

The surface composition of the conducting polymer film also can be modified by additives.^[3–6] The PSS-to-PEDOT ratio at the surface can be controlled by adding more PSS molecules with low molecular weight PSS ($M_w = 48,000$) instead of high molecular weight PSS ($M_w = 490,000$), and with more volatile methanol solvent instead of water (Figure 9d,e); as a result, the WF increases from 5.20 eV to 5.44 eV (Figure 9f).^[3] Basically, because PEDOT:PSS is highly p-doped, the Fermi level of PEDOT:PSS is expected to be close to the filled states, but inverse photoemission spectroscopy combined with ultraviolet photoemission spectroscopy (IPES/UPS) analysis revealed that the Fermi level of PEDOT:PSS is near the middle of the bandgap due to effect of long insulating PSS chains at the surface of PEDOT:PSS film.^[244] The surface concentration of PSS in PEDOT:PSS film was gradually increased by increasing the concentration of PSS molecules added to commercially-available PEDOT:PSS solution (Figure 9d).^[244] These changes indicate that the surface WF of PEDOT:PSS film can be increased by using a surface-enriched PSS layer and also can be controlled by adjusting the amount of the additional PSS (Figure 9f). Effective WF tuning of the conducting polymer was demonstrated by adding polymeric acid that has low surface energy, perfluorinated ionomer (PFI), tetrafluoroethylene-perfluoro-3,6-dioxo-4-methyl-7-octanesulfonic acid copolymer (NafionTM), to PEDOT:PSS solution (Figure 9g).^[4,5] The PFI has fluorocarbons in its molecular structure and therefore has much lower surface energy ($\approx 20 \text{ mN m}^{-1}$) compared with that of PEDOT:PSS (ca. $71\text{--}73 \text{ mN m}^{-1}$)^[245]; as a result, PFI molecules self-organize to be preferentially positioned at the top surface of PEDOT:PSS:PFI film facing air, which was evidenced by molecular depth profiles for PEDOT:PSS:PFI film (Figure 9h).^[4,5] The PFI has high ionization potential. Gradual increase of PFI molecular concentration from bottom to top surface of the film

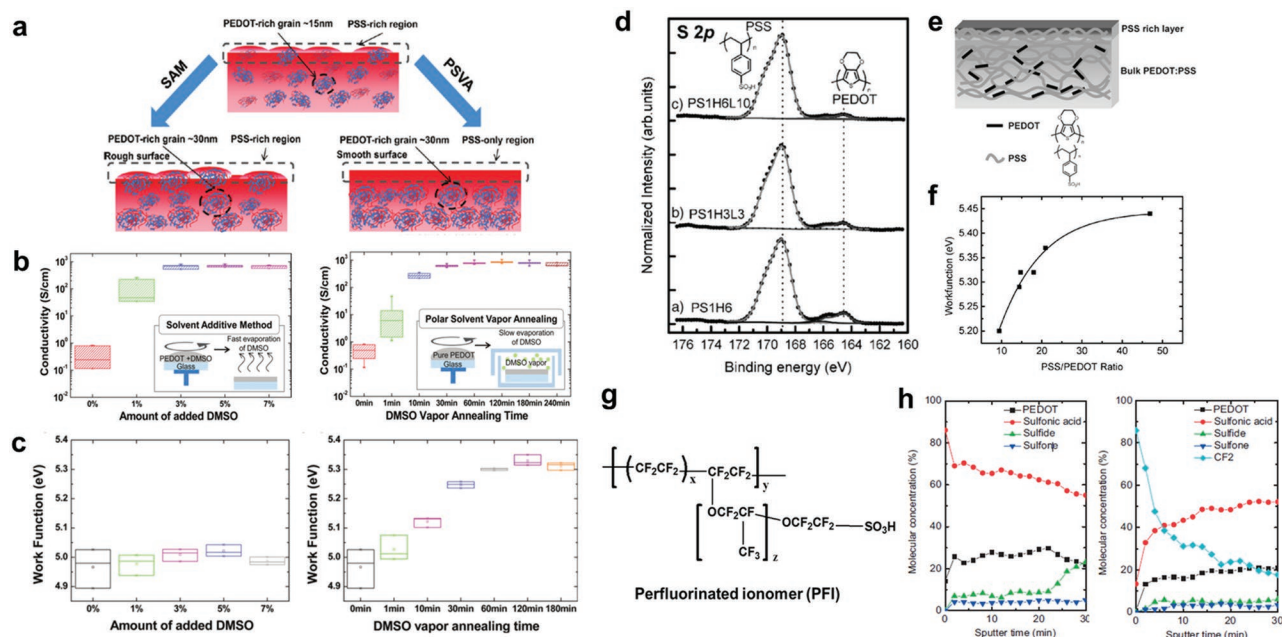


Figure 9. Material engineering to increase WF of the conducting polymer. a) Schematic morphological models of spin-coated pristine, solvent additive method (SAM)-treated, and polar solvent vapor annealing (PSVA)-treated PEDOT:PSS films. b) Conductivity and c) work function of PEDOT:PSS films treated using the SAM with various amounts of added DMSO, and using PSVA with various annealing times. a–c) Reproduced with permission.^[218] Copyright 2012, American Chemical Society. d) S 2p core level spectra of the PEDOT:PSS with varying the PSS compositions. e) Schematic morphology of spin-cast PEDOT:PSS films. f) The effect of PSS/PEDOT ratio at the film surface on the film work function. d–f) Reproduced with permission.^[3] Copyright 2008, WILEY-VCH. g) Molecular structure of PFI and h) molecular depth profiles for the anode buffer layers of PEDOT:PSS (left) and PEDOT:PSS:PFI (right). Deconvoluted S 2p peaks for PEDOT, sulfonic acid, sulfide, and sulfone concentrations and C 1s peak at 292 eV for the PFI concentration were used. g,h) Reproduced with permission.^[4] Copyright 2007, WILEY-VCH.

implies that ionization potential increases gradually across the film and that its surface ionization potential becomes high. The surface WF can be tuned to >5.9 eV by controlling the ratio of PFI to PEDOT:PSS.^[5,6,30,31] This approach achieves a conducting polymer-based anode buffer layers with a wide-range controllable WF.

The PFI molecules at the film surface also prevent exciton quenching at the interface between PEDOT:PSS and the overlying semiconducting layers, which was evidenced by increased photoluminescence (PL) intensity and extended PL lifetime.^[5,8] The PEDOT:PSS:PFI anode buffer layer has excellent hole-injection capability and exciton quenching-blocking capability in the organic, polymer, and OIHP LED devices.

Use of PEDOT:PSS:GO composite as an anode buffer layer is another way to reduce exciton quenching at the interfaces due to the large bandgap (≈ 3.6 eV) of the GO in the composite.^[246] The exciton lifetime of organic light-emitting layer on PEDOT:PSS:GO layer was about three times longer than that on PEDOT:PSS.

Water-soluble self-doped conducting polymer (SCP)-based anode buffer layer is a possible alternative to water-dispersible PEDOT:PSS (Figure 10a). SCP has unique and advantageous properties such as water solubility and chemical stability due to the charged functional groups (dopants), covalently bound to the conducting polymer backbone (Figure 10b).^[100,102] SCPs have covalently bound dopants; therefore the phase separation does not occur and they have high stability during storage and excellent film-forming property.^[39,100–102] They are also stable

in a wide range of pH, whereas PEDOT:PSS loses its dopants at high pH, resulted from the de-doping process.^[209–212] The stable nature of self-doped PEDOT (PEDOT-SO₃H) and PSS grafted PANI (PSS-g-PANI) (Figure 10b,c) contributed to increase the efficiency and lifetime of the devices that use them as anode buffer layers.^[9,247] When a water-soluble conducting polymer, PEDOT-SO₃H, was used as a recombination layer of bulk-heterojunction tandem SCs, the device life time was prolonged. The device with PEDOT-SO₃H maintained about 75% of its initial PCE after 100 h, whereas the device with the PEDOT:PSS showed a fast degradation of PCE to <30% of its initial efficiency in 40 h.^[247] The another water-soluble conducting polymer, PSS-g-PANI, demonstrated its higher stability in OLEDs and OSCs, compared to PEDOT:PSS.^[9] The device half-lifetime, time required for the luminance to decrease to half of its initial value, of OLEDs with Beq₂C545T emitting layer was increased from 7.6 h to 55 h when the anode buffer layer was changed from PEDOT:PSS to PSS-g-PANI.^[9] Replacing PEDOT:PSS with PSS-g-PANI in OSCs that have a P3HT:PCBM photoactive layer increased the device half-life-time from 186 h to 267 h.^[9]

Processability and stability of polymeric anode buffer layers are important features that must be achieved to make commercialization of organic and OIHP optoelectronic devices feasible. In this regard, water-soluble SCP has advantages over the conventional water-dispersible conducting polymers; and therefore the SCP is a promising material for use as a stable and efficient anode buffer layer for optoelectronic devices.

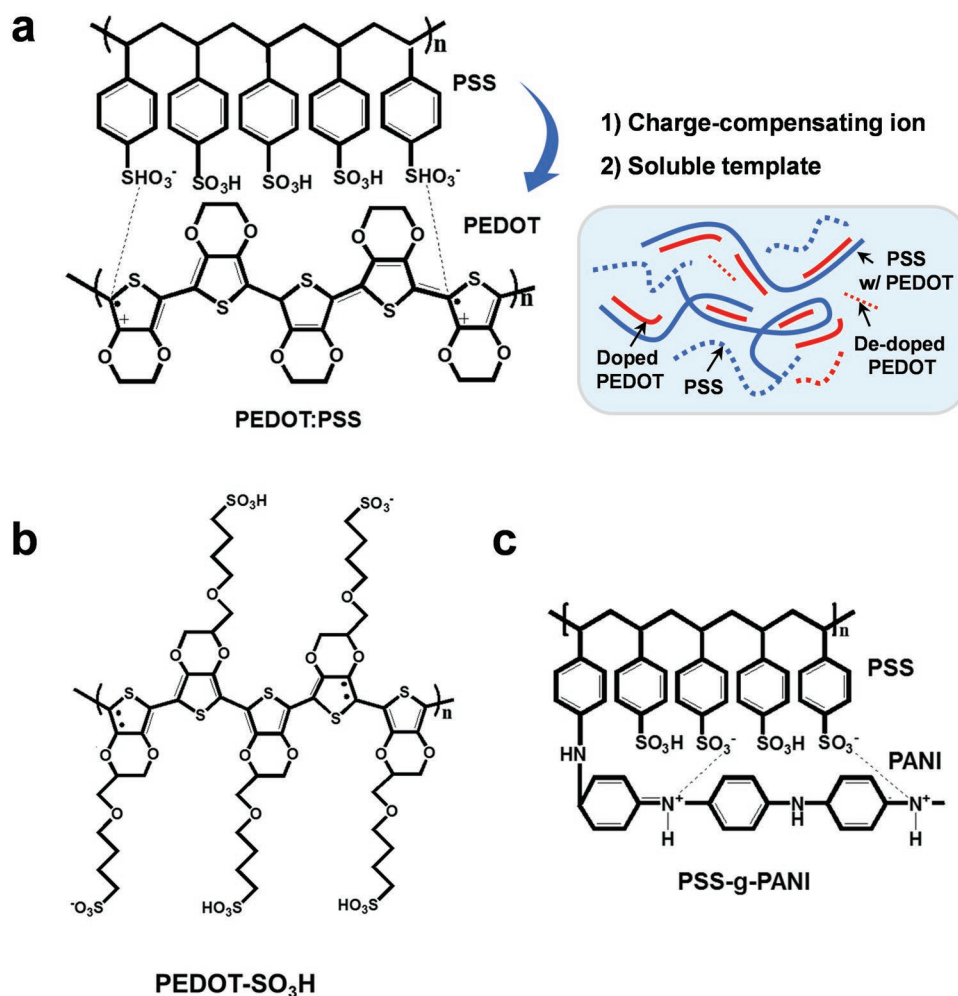


Figure 10. Molecular structures of a) water-dispersible HIL, PEDOT:PSS, and water-soluble HILs, b) PEDOT-SO₃H and c) PSS-g-PANI.

3. Conducting Polymer-Based Anode Buffer Layers in Light-Emitting Diodes

OLEDs and PeLEDs emit light as a result of radiative recombination of charge carriers that are injected from the cathode and the anode.^[248] OLEDs use organic compounds as emissive layers, whereas PeLEDs use OIHP materials.^[29–31] OLEDs have been successfully commercialized and have advantages of low power consumption, light-weight and large viewing angle. Both vacuum process and solution process technologies can be applied to fabricate films of organic compound emitters. Also, the feasibility of flexible and stretchable devices make OLEDs a fascinating research area.

OIHPs have outstanding light absorption, small exciton binding energy and excellent exciton confinement, so they provide alternatives to organic materials in optoelectronics.^[29,30,249] OIHPs also have the advantage of low-cost solution processability.^[29–32,37] Three dimensional OIHP is composed of ABX₃ units (where A is an organic cation, B is a divalent metal ion and X is a halide). By simply changing the halide (e.g. Br, Cl, I), the energy band gap of OIHPs can be easily tuned.^[30] The feasibility of using OIHPs in optoelectronics was first demonstrated

in SCs^[40,250] and recently in LEDs.^[29–31] Especially, the high color purity of OIHPs makes PeLEDs promising as next-generation light-emitting sources to replace conventional LEDs. PeLEDs have been spotlighted due to low material cost compared with OLED devices. Moreover, solution processable OIHPs enable low-cost printing fabrication even on large-areas.

In OLEDs, the external quantum efficiency (EQE, η_{EQE}) is used to evaluate the luminous efficiency of OLEDs.^[251] EQE is the ratio of the number of photons emitted from devices to the number of charge carriers injected from both electrodes:

$$\eta_{\text{EQE}} = \chi \eta_{\text{IQE}} = \chi \gamma \beta \phi_{\text{L}}$$

where χ is out-coupling factor, η_{IQE} is internal quantum efficiency, γ is charge balance factor, β is the probability of production of emissive species, and ϕ_{L} is quantum efficiency of luminescence. χ is determined by the light out-coupling structures of devices, and can be increased by using various light out-coupling techniques including substrate modification to increase light-extraction from devices. Theoretically, η_{IQE} for fluorescent organic dyes is limited to <0.25 because the radiative decay of triplet excitons is forbidden.^[252,253] However,

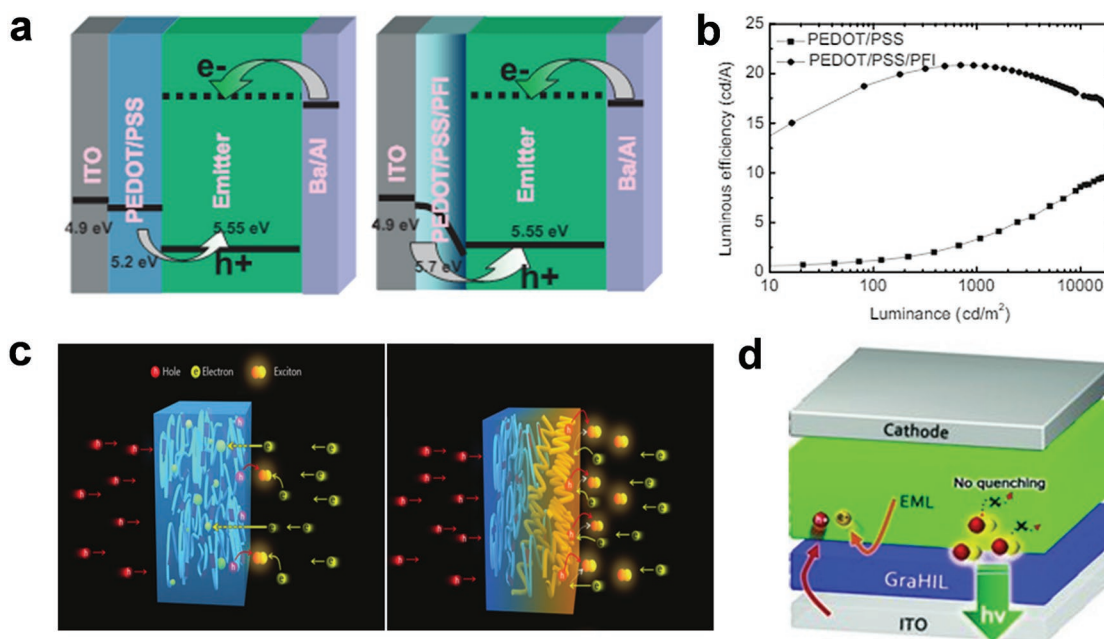


Figure 11. a) Schematic band diagram and b) luminous efficiency versus luminance curve of PLEDs with PEDOT:PSS:PFI hole injection layer. a,b) Reproduced with permission.^[4] Copyright 2007, WILEY-VCH c) Schematics of self-organized PFI in hole injection layer regarding capability to inject holes, blocking electrons and quenching of excitons, d) device structure of small-molecule OLEDs with simplified structures. c,d) Reproduced with permission.^[5] Copyright 2012, WILEY-VCH.

phosphorescent organic dyes allow η_{IQE} to be 1. They enable intersystem crossing (ISC) between singlet and triplet excitons by exploiting the spin-orbit interaction of heavy metal atoms such as iridium and platinum.^[254–256] Recently, thermally-activated delayed fluorescence (TADF) dyes have been reported;^[257] they have very small energy difference between singlet and triplet excitons, allow reverse-ISC, and therefore can theoretically achieve η_{IQE} of ≈ 1 . However, to approach η_{IQE} of ≈ 1 , charge carrier injection from electrodes to emissive layers and charge carrier balances in emissive layers must be improved. Efficient OLEDs use multilayer structures to improve charge carrier injection and charge balance. Especially, to overcome the high energy barrier between anode and overlying organic semiconducting layer and to facilitate charge injection to this layer, various anode buffer layers have been introduced in OLEDs and PeLEDs.^[4,45,54–61,71,72,187,237]

Basically, anode buffer layers based on conducting polymers circumvent the disadvantages of underlying anodes, especially their low WF. The widely used conducting polymer-based anode buffer layer materials (e.g., PEDOT:PSS and PANI:PSS) have insufficient WF ≈ 5.2 eV to make Ohmic contact to organic semiconducting layers.^[3,100]

Among various approaches to tune WF of PEDOT:PSS-based anode buffer layer, the most effective way is to add PFI.^[4–6,30,37,38] The surface WF of PEDOT:PSS:PFI film was gradually increased up to 5.95 eV as the ratio of PFI to PEDOT:PSS increased.^[4] When PEDOT:PSS:PFI film was used as an anode buffer layer in a green PLEDs based on a polyfluorene derivative (Figure 11a), the current efficiency (CE) was 21 cd A⁻¹, which is much higher than that of the device employing conventional PEDOT:PSS buffer layer (9.8 cd A⁻¹) (Figure 11b).^[4]

The PEDOT:PSS:PFI system was also used for solution-processed OLEDs based on a thermally cross-linkable bipolar host and dopant system to improve the hole injection from anode to emitting layer.^[258] The device employing the PEDOT:PSS:PFI anode buffer layer showed a maximum CE of 15.3 cd A⁻¹.

A bilayer system, PEDOT:PSS/PFI, was also used to reduce the hole injection barrier between anode and overlying hole transport layer.^[259] The PFI layer was over-coated on the PEDOT:PSS layer, and the resultant WF of the PEDOT:PSS/PFI bilayer film was increased up to 5.64 eV (4.94 eV for the pristine PEDOT:PSS). The green phosphorescent OLEDs using the PEDOT:PSS/PFI as an anode buffer layer showed the CE of 33.6 cd A⁻¹, which was higher than that using the pristine PEDOT:PSS (29.2 cd A⁻¹). The higher CE was attributed to the well-aligned WF of the PEDOT:PSS/PFI layer to the HOMO energy level of NPB, resulting in the improved hole injection and reduced driving voltage.

PFI also increased the WF of anode buffer layers based on a self-doped conducting polymer, PSS-g-PANI (Figure 10c).^[9] In PSS-g-PANI films, the PFI increased the surface WF to as much as 6.09 eV.^[9] Also, the hole injection efficiency $\eta_{Injection}$ was calculated by using theoretical space charge limited current (SCLC) with hole-only devices. As the WF increased, $\eta_{Injection}$ was increased to ≈ 1.0 , which means nearly-Ohmic contact with the overlying semiconducting layer.^[9] When the blend of PSS-g-PANI and PFI was used as an anode buffer layer in fluorescent OLEDs, the CE increased to 19.4 cd A⁻¹. Moreover, the lifetime of the devices (290 h) was 38 times longer than that of the devices that used PEDOT:PSS-based anode buffer layers (7.6 h); this improvement was attributed to the synergistic effect of

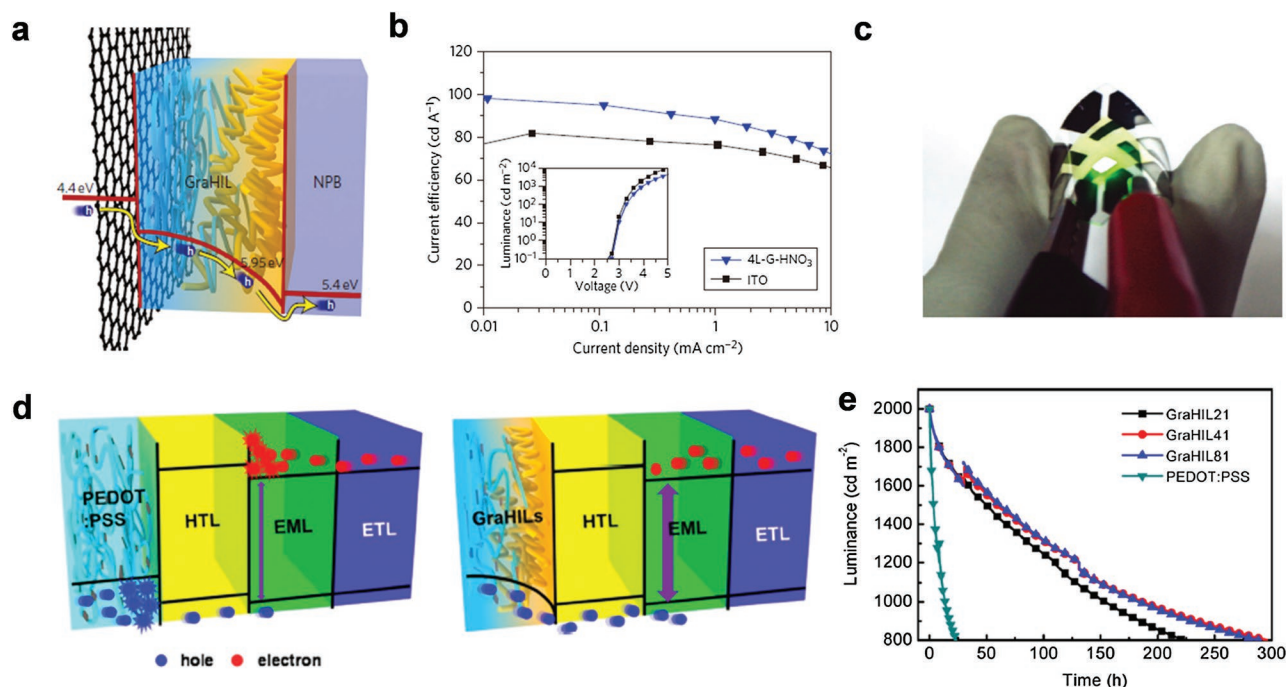


Figure 12. a) Schematic illustration of the self-organized hole injection buffer layer on graphene anode, b) current efficiency versus current density of flexible OLEDs with the graphene anode. c) Optical image of light emission from a flexible fluorescent green OLED on graphene anode. a–c) Reproduced with permission.^[6] Copyright 2012, Nature Publishing Group. d) Degradation mechanism of OLEDs and e) operational lifetimes of OLEDs according to hole injection buffer layers. d,e) Reproduced with permission.^[8] Copyright 2015, American Chemical Society.

intrinsic chemical stability of PSS-g-PANI and an excellent diffusion barrier property of PFI.^[4,9]

Furthermore, the enrichment of PFI molecules at the surface prevents exciton quenching at the interface between the conventional anode buffer layer (e.g. PEDOT:PSS) and the organic semiconducting layer (Figure 11c).^[4,5] Insulating PFI can effectively block electrons and excitons that are transported from the organic emitting layer. As the ratio of PFI to PEDOT:PSS increases, the PL lifetime of the emissive layer measured by the time-correlated-single-photon-counting was gradually increased.^[5] A highly-efficient hole-injection buffer layer composed of PEDOT:PSS:PFI allowed simplification of device structure in OLEDs: because the hole-injection buffer layer itself provides efficient hole injection, good electron blocking, and prevention of exciton quenching, additional functional layers such as HTL or electron blocking layer (ETL) can be omitted in the simple-device structure that uses PEDOT:PSS:PFI (Figure 11c,d).^[5] With simple device structure that uses only one vacuum-deposited organic emitting layer on top of the solution-processed hole injection buffer layer, the current efficiency was comparable to that of a multilayered device that used both HTL and ETL.

Polymeric hole injection buffer layers have also been used to modify electrical properties of underlying anode materials. Graphene has potential as a flexible transparent electrode due to its unique electrical properties, excellent mechanical flexibility, and high transmittance.^[6,260–263] However, graphene has lower WF (≈ 4.4 eV) than ITO anode (≈ 4.7 – 4.9 eV),^[3,166–170] so the hole injection energy barrier between graphene anode and overlying organic layers is large. A polymeric hole injection

buffer layer composed of PEDOT:PSS:PFI on graphene anode can overcome this large energy barrier for hole injection (Figure 12a).^[6] Self-organization of polymer chains in the buffer layer causes an increasing gradient WF from anode to organic layer; this and the high surface WF of the graphene anode buffer layer causes Ohmic contact between graphene anode and the hole transporting layer (Figure 12a). As a result, the flexible OLEDs with graphene anode exhibited very high luminous efficiencies (≈ 98.1 cd A⁻¹, 102.7 lm W⁻¹), which exceed those obtained using a conventional rigid ITO anode (≈ 81.8 cd A⁻¹ and 85.60 lm W⁻¹) (Figure 12b,c).^[6]

Because the surface WF of the polymeric hole injection layer gradually increases as PFI concentration increases in the PEDOT:PSS, the energy barrier between anode and hole transporting layer is also reduced; as a result, hole injection into the layers is improved. In contrast, the low WF of the conventional PEDOT:PSS buffer layer gives it inefficient hole injection.^[8] The result is that hole carriers that were not injected, and counter charges that have not recombined with holes accumulate at interfaces between layers; these space charges trap charges and cause non-radiative recombination, thereby decreasing the electrical and electroluminescent properties of OLEDs (Figure 12d,e).^[8]

The enrichment of PFI at the surface of the buffer layer can effectively block metal ions that diffused from the ITO anode. Therefore, use of a polymeric buffer layer can effectively prevent undesired charge trapping and exciton quenching that are caused by impurities.^[8] OLEDs that use PEDOT:PSS:PFI have higher luminous efficiency and 10 times longer operational lifetimes than OLEDs that use PEDOT:PSS.^[8]

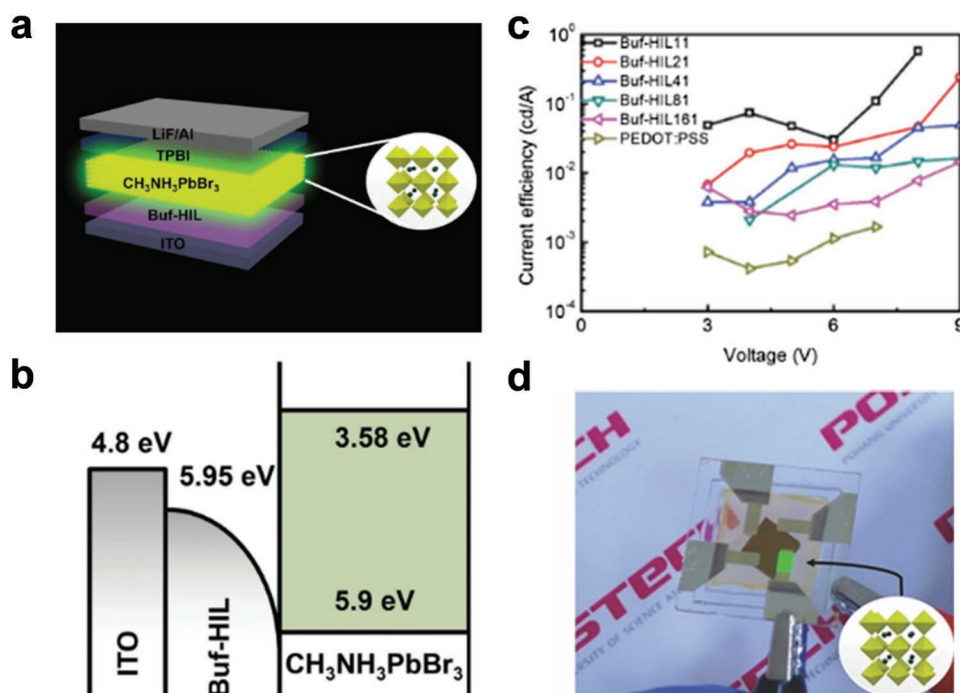


Figure 13. a) Schematic device structure and b) energy band diagram of the PeLED. c) Current efficiency versus voltage curves of PeLEDs depending at different ratios of PFI to PEDOT:PSS. d) Uniform illumination of the PeLED. a–d) Reproduced with permission.^[30] Copyright 2014, WILEY-VCH.

In PeLEDs, the problem of low WF of anodes and exciton quenching at the interface between anode and emissive layer is more serious than in OLEDs. The most commonly-used green-emission OIHP emitter is methyl ammonium lead bromide $\text{CH}_3\text{NH}_3\text{PbBr}_3$ (MAPbBr₃), which emits green light stably even at RT. However, it has very deep VBM of 5.9 eV, which is much deeper than the HOMO energy level of organic semiconducting layer.^[30,31] Therefore, anode buffer layers should have high WF to facilitate hole injection from anode to overlying emitting materials. Also, low exciton binding energy and long exciton diffusion length (ca. 100–1000 nm)^[249,264,265] of OIHPs cause severe exciton quenching at the interface between anode and OIHP layer. Therefore, to improve the CE of PeLEDs, the large hole-injection barrier and exciton quenching in PeLED applications must be overcome.

One possible solution is to use an anode buffer layer that can reduce the hole injection barrier and prevent exciton quenching at the interface between anode and emissive layer. A multi-functional conducting polymer-based anode buffer layer was introduced to solve these problems (Figure 13).^[30] Also, the enrichment of insulating PFI at the surface can effectively block exciton quenching between the anode buffer layer and the MAPbBr₃ layer; as a result, and the resultant PL lifetime was greatly extended.^[30] The PL lifetime of MAPbBr₃ on top of the PEDOT:PSS:PFI buffer layer was increased to 4.7 ns, whereas that of MAPbBr₃ on top of pristine PEDOT:PSS was 0.34 ns. These two effects of the multi-functional anode buffer layer increased the CEs of PeLEDs as the ratio of PFI to PEDOT:PSS in the anode buffer layer increased (Figure 13c). The maximum CE of the PeLED that used a PEDOT:PSS:PFI anode buffer layer (0.577 cd A⁻¹) was 350 times higher than that of the device that

used a pristine PEDOT:PSS anode buffer layer (Figure 13d).^[30] Recently, a highly conductive PEDOT:PSS:PFI, where a polar solvent, DMSO, was added to increase the electrical conductivity of the film, was also used as an anode for MAPbBr₃-based PeLED. The resultant maximum CE was 42.9 cd A⁻¹, which is the highest CE among the reported PeLEDs that emit visible light.^[31]

The results confirm that the PEDOT:PSS:PFI buffer layer can be applied to various types of LEDs, including OLEDs and PeLEDs. Reported LEDs have efficiencies and lifetimes that depend on the type of conducting polymer-based anode buffer layers (Table 1). Use of multi-functional conducting polymer-based anode buffer layers greatly increased the maximum CE and lifetime regardless of the emissive layer used. The results confirm the importance of anode buffer layer engineering.

4. Conducting Polymer-Based Anode Buffer Layers in Solar Cells

SCs converts light energy into electrical power. When photoactive layers absorb light, electron/hole pairs (excitons) are generated. By the built-in potential between anode and cathode, the electron/hole pairs are separated, and the separated electrons and holes are collected at the cathode and anode, respectively.^[207] OSCs use organic small molecule or polymer photoactive materials, whereas PeSCs use OIHP materials as photoactive materials. Both OSC and PeSC have the advantages of low-cost solution processability. Especially, OSCs have possible uses as stretchable devices when polymer materials are used as photoactive layers.^[266–268] OIHPs have outstanding light absorption,

Table 1. Summary of LED performances depending on conducting polymer-based anode buffer layers.

Anode/conducting polymer-based anode buffer layers	Device architecture	Max. CE ^{a)} [cd A ⁻¹]	Max. EQE ^{b)} [%]	Device lifetime ^{c)} [h]	Color	Ref.
ITO/PEDOT:PSS	NPB/Alq ₃ :C545T/Alq ₃ /Al	14.7	3.88		Green	[236]
ITO/MoO ₃ /PEDOT:PSS		23.4	6.31			
ITO/PEDOT:PSS	Super Yellow/LiF/Al	11.3		41.5	Yellow	[271]
ITO/PEDOT:PSS: MoO ₃		13.5		108.1		
ITO/PEDOT:PSS	TPD/CBP:Ir(ppy) ₃ /Bphen/Liq/Ca/Al	42			Green	[274]
ITO/PEDOT:PSS:GO		52	-			
ITO/PEDOT:PSS	Super Yellow/LiF/Al	10.04	3.58		Yellow	[246]
ITO/PEDOT:PSS:GO		21.74	7.48			
ITO/PEDOT:PSS	polyfluorene derivative/Ba/Al	21			Green	[4]
ITO/PEDOT:PSS:PFI		9.8				
ITO/PEDOT:PSS	NPB/Bebq ₂ :C545T/Bebq ₂ /Liq/Al	15.0		7.6	Green	[9]
ITO/PANI:PSS		15.5		4.8		
ITO/PSS-g-PANI		15.9		55		
ITO/PSS-g-PANI:PFI		19.4		290		
ITO/2TNATA	Bebq ₂ :C545T/Liq/Al	12			Green	[5]
ITO/PEDOT:PSS:PFI		20				
ITO/PEDOT:PSS:PFI	TAPC/TCTA:Ir(ppy) ₃ /CBP:Ir(ppy) ₃ :TPBi/LiF/Al	81.8			Green	[6]
Graphene/PEDOT:PSS:PFI		98.1				
ITO/PEDOT:PSS	NPB/Bebq ₂ :C545T/Bebq ₂ /LiF/Al	15.2		25	Green	[8]
ITO/PEDOT:PSS:PFI		17.3		300		
ITO/PEDOT:PSS	CH ₃ NH ₃ PbBr ₃ /TPBi/LiF/Al	0.00165	0.000393		Green	[30]
ITO/PEDOT:PSS:PFI		0.577	0.125			
ITO/PEDOT:PSS:PFI	DVB-CzDTAZ:Ir(mppy) ₃ /TPBi/Liq/Al	15.3			Green	[258]
ITO/PEDOT:PSS	NPB/CBP:Ir(ppy) ₃ /BALq/Alq ₃ /LiF/Al	29.2	14.1		Green	[259]
ITO/PEDOT:PSS:PFI		33.6	16.2			

^{a)}Max. CE: maximum current efficiency; ^{b)}Max. EQE: maximum external quantum efficiency; ^{c)}Device Lifetime: device half-lifetime

small exciton binding energy, and long exciton diffusion length; as a result, they have increased the PCE of SCs to 22.1%.^[269]

Open-circuit voltage (V_{oc}) is particularly dependent on the energy level alignment in SCs, and is mainly determined by the WF difference between anode and cathode when both electrodes make Ohmic contact with active layers.^[207] V_{oc} decreases when energy level offset increases between photoactive layers and electrodes.^[40] Therefore, to increase V_{oc} , interfacial buffer layers must be used to achieve Ohmic contact between photoactive layers and electrodes.

To align the energy levels of the buffer layer with those of the semiconducting layers, and to achieve efficient charge extraction and high V_{oc} , transition metal oxides have been widely used as an anode buffer layer in OSCs and PeSCs.^[43,70,72,74] However, transition metal oxides are fabricated using an expensive vacuum process or high-temperature annealing, so their use is not compatible with the goal of low-cost solution-printing.

Conducting polymers have also been used as anode buffer layers in SCs, but have low WF (e.g. PEDOT:PSS, ClevisTM PH has WF of ≈ 4.86 eV),^[37,38] which limit the V_{oc} of SCs. The WF manipulation of conducting polymer anode buffer layers resulted in improvement of the SC characteristics.^[37-39]

The most widely-used photoactive OIHP material in PeSCs is methyl ammonium lead iodide (CH₃NH₃PbI₃, MAPbI₃).^[37-40,195,201] The difference between the VBM of MAPbI₃ (≈ 5.4 eV),^[37] and the WF of PEDOT:PSS (≈ 4.86 eV for ClevisTM PH) is too high to allow Ohmic contact between the layers.^[37,38] As we explained in previous chapters, addition of a small amount of PFI can effectively tune the surface WF of PEDOT:PSS; due to the surface energy difference, the PFI molecules become enriched on the film surface. A small amount of PFI increased the surface WF of hole extraction layer to 5.39 eV (Figure 14a),^[37] which is comparable to the ionization potential of MAPbI₃ (Figure 14b). The PeSC that used PEDOT:PSS:PFI as an anode buffer layer had PCE of 11.7%, whereas the device with conventional PEDOT:PSS buffer layer showed PCE of 8.1%.^[37] The increase in the PCE was attributed to increase in the V_{oc} , fill factor (FF) and short-circuit current density (J_{sc}). The increased V_{oc} confirmed the effect of the increased WF of the polymeric anode buffer layer. Also, the increases in V_{oc} , FF and J_{sc} were related to the increase in the built-in potential (V_{bi}). The PeSCs that used the PEDOT:PSS:PFI anode buffer layer produced the increased photocurrent difference between under illumination and in

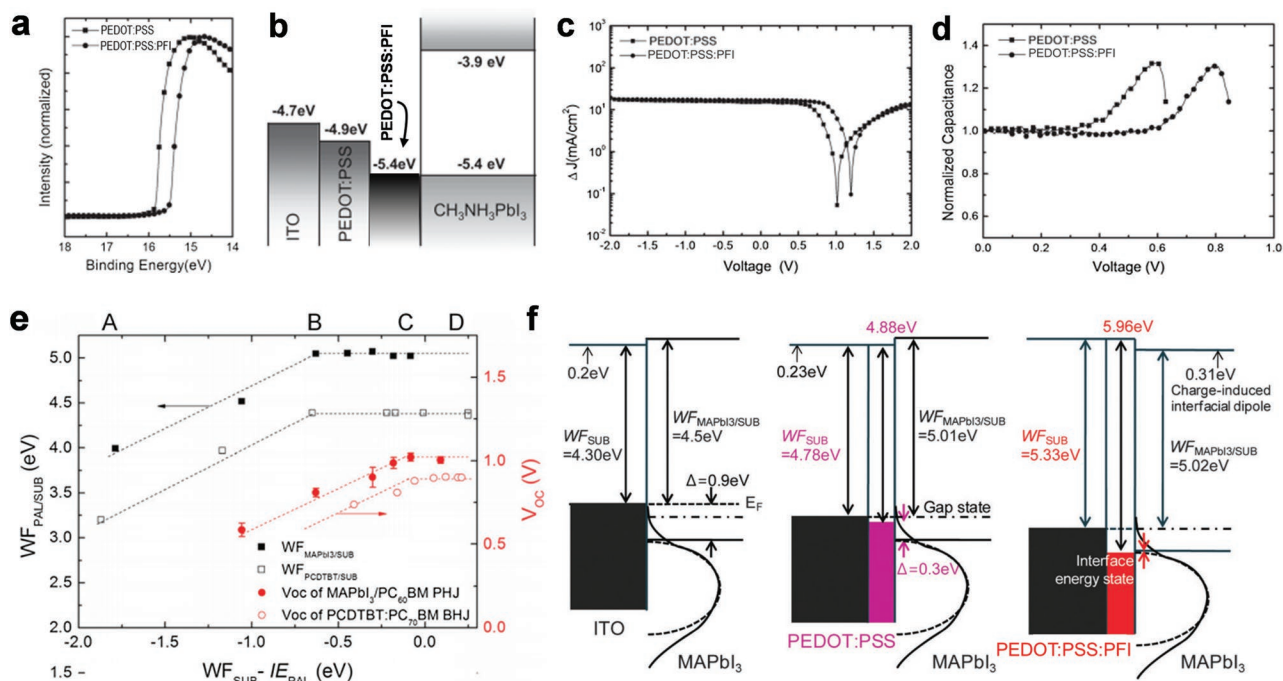


Figure 14. a) Increase in work function by adding PFI. b) Schematic energy band diagrams of PeSC. c) Difference Δj of photocurrent under illumination and in the dark for ITO/PEDOT:PSS:PFI/ $\text{CH}_3\text{NH}_3\text{PbI}_3$ /PCBM/Al device (circles) and ITO/PEDOT:PSS/ $\text{CH}_3\text{NH}_3\text{PbI}_3$ /PCBM/Al device (squares). d) Capacitance–voltage characteristics of devices depending on anode buffer layers. a–d) Reproduced with permission.^[37] Copyright 2014, WILEY-VCH. e) Open circuit voltage of the PeSCs (filled) and OSCs (open) depending on the difference of the work function of conducting substrates and VBM of the photoactive layer. f) Schematic energy band diagrams depending on interface energy state of polymeric anode buffer layers (PEDOT:PSS and PEDOT:PSS:PFI). e, f) Reproduced with permission.^[38] Copyright 2016, Royal Society of Chemistry.

the dark due to the increased V_{bi} (Figure 14c). The increased V_{bi} means the increase of forward diffusion of photogenerated carriers and internal electrical field in the PeSC that used PEDOT:PSS:PFI; The increased V_{bi} was also confirmed by the capacitance–voltage (C–V) characteristics (Figure 14d).

The WF-tuning of conducting polymer-based anode buffer layer can be applicable for various SCs, not only PeSCs but also OSCs.^[38] As in the MAPbI_3 -based PeSCs, the PCEs of the PCDTBT-based OSCs were improved when the high-WF PEDOT:PSS:PFI anode buffer layer was used (6.3% for PEDOT:PSS:PFI; 4.2% for PEDOT:PSS).^[38] The improved PCEs in the device were attributed to increase of the V_{bi} , which resulted in the increase in V_{oc} , J_{sc} , and FF. In addition to the PCE improvement, the PEDOT:PSS:PFI system greatly prolonged the lifetime of the OSCs from 300 h to 4700 h.^[38] As we discussed in the OLEDs that use self-organized polymeric anode buffer layer, the improved lifetime also can be attributed to the ability of the PEDOT:PSS:PFI to block diffusion of impurities^[38]; the enrichment of PFI molecules at the surface prevents the diffusion of impurities (e.g., sulfates, alkali metals, In atoms, and Sn atoms) into the overlying active layer.

The universal energy level tailoring in the hole extraction interface of OSCs and PeSCs was observed. V_{oc} was measured in SCs with the following photoactive layers: (1) MAPbI_3 / [6,6]-Phenyl C61 butyric acid methyl ester (PC_{60}BM) in PeSCs (2) poly[*N*-9'-heptadecanyl-2,7-carbazole-*alt*-5,5-(4',7'-di-2-thienyl-2',1',3'-benzothiadiazole)] (PCDTBT): [6,6]-Phenyl C71 butyric acid methyl ester (PC_{71}BM) for OSCs. Then V_{oc} was plotted versus the difference between the WF of the conducting

substrate (glass/Al (3.4 eV), ITO/1-octadecanethiol (ODT) self-assembled monolayer (4.1 eV), PEDOT:PSS:PFI (4.6–5.5 eV)) and the ionization energy of the overlying photoactive layer (Figure 14e).^[38] At a certain WF of the conducting substrate, the WF of the photoactive layer on the substrate stopped increasing at the level of ≈ 0.6 – 0.7 eV above the HOMO energy level of PCDTBT or VBM of MAPbI_3 : This implies Fermi-level at the interface was pinned. However, the resultant V_{oc} still increased until the ionization energy of photoactive layer is almost equal to the substrate WF. This further increase of V_{oc} can be ascribed to modulation of the interface energy state caused by surface enriched PFI layer on top of the PEDOT:PSS:PFI layer (Figure 14 f). As a result, the potential energy loss at the hole extraction interface can be minimized and thus the V_{oc} can be maximized in the OSCs and PeSCs using PEDOT:PSS:PFI anode buffer layer.^[38]

A DMSO-treatment has been reported to effectively improve the electrical conductivity of PEDOT:PSS:PFI films. After the film formation of PEDOT:PSS:PFI, the films were fluxed by DMSO, and then annealed. With the increased WF by PFI, the DMSO-treated PEDOT:PSS:PFI film facilitated the charge collection in PSCs. As a result, the PSCs showed the increased J_{sc} of 22.10 mA cm^{-2} , improving the PCE up to 9.82% (the J_{sc} of 14.31 mA cm^{-2} and the PCE of 7.35% for the PSC using the pristine PEDOT:PSS).^[270]

Water soluble conducting polymer, PSS-g-PANI, was also modified to have increased surface WF by addition of PFI (Figure 15a).^[39] The resultant surface WF of PSS-g-PANI:PFI was 5.49 eV, which is high enough to form Ohmic contact with

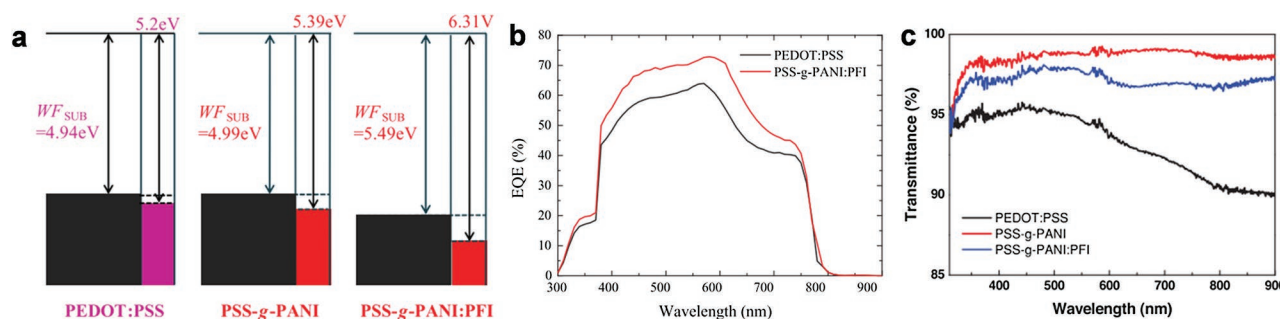


Figure 15. a) Schematic energy band diagrams of PEDOT:PSS, PSS-g-PANI, and PSS-g-PANI:PFI. b) EQE spectra of the PeSCs with PEDOT:PSS and PSS-g-PANI:PFI. c) Transmittance of PEDOT:PSS, PSS-g-PANI, and PSS-g-PANI:PFI. a–c) Reproduced with permission.^[39] Copyright 2016, WILEY-VCH.

OIHP layers (e.g. MAPbI₃ has ionization energy of 5.43 eV).^[39] The PSS-g-PANI:PFI film was used as a hole extraction anode buffer layer for PeSCs that had the MAPbI₃ photoactive layer. The PSS-g-PANI:PFI-based PeSC had PCE of 12.4%, whereas the device that used conventional PEDOT:PSS had PCE of 7.8%, and the device that used PSS-g-PANI had PCE of 9.7%.^[39] The V_{bi} was increased by using the PSS-g-PANI:PFI as an anode buffer layer in PeSCs, and thus PCE was also increased. Also, the improved EQE according to wavelength of the PeSCs with PSS-g-PANI:PFI (Figure 15b) revealed that the higher transmittance of PSS-g-PANI (Figure 15c) also can be an additional reason for improvement of the device efficiency compared with that of conventional PEDOT:PSS.^[39]

One of the demerits of conventional PEDOT:PSS as the anode buffer layers for graphene anode-based flexible OSCs is the poor wetting of hydrophilic PEDOT:PSS on a non-polar and hydrophobic graphene surface (Figure 16a). The composite hole extraction buffer layers can be used for overcoming this critical impediment in the graphene anode-based OSCs.^[271] Due to the hydrophobic nature of fluorine containing polymer, PFI, the PEDOT:PSS:PFI hole extraction buffer layer was uniformly formed on top of the graphene anodes (Figure 16b). By additionally optimizing the number of graphene layers, the graphene anode-based OSC that used poly(3-hexylthiophene-2,5-diyl) (P3HT) had PCE of 2.83%, and when PCDTBT was used as a photoactive material, the PCE was reached to 4.33%.^[271]

The surface energy of the anode buffer layer can additionally have influence on morphology of overlying active layers in solar cells. In OSCs, it has been reported that the surface energy of anode buffer layer influences the phase separation of

the P3HT:PCBM blends.^[272] It is also reported that the surface energy of underlying buffer layers determines the grain size of overlying perovskite active layers in PeSCs. The grain size of CH₃NH₃PbI₃ film significantly decreased as the surface energy of the anode buffer layer increased.^[273] Therefore, the well-matched surface energy of anode buffer layer with an overlying active layer can be considered as an additionally requirement for efficient SCs.

Material engineering of conducting polymer-based anode buffer layers including PEDOT:PSS:MoO₃, PEDOT:PSS:GO, PEDOT:PSS:PFI, and PSS-g-PANI:PFI has been used to improve the photovoltaic efficiency and stability of SCs regardless of the photoactive materials used. Reported PCEs and lifetimes depending on the type of conducting polymer-based anode buffer layers are summarized in Table 2.

5. Conclusions

This review has presented the importance of anode buffer layers in organic and OIHP optoelectronic devices including LEDs and SCs. The primary function of anode buffer layers is to align the energy level by reducing the energy level offset between anodes and overlying semiconducting layers; by accomplishing these goals, device efficiency and stability are increased. The anode buffer layers must have (1) high WF enough to form Ohmic contact with an overlying semiconducting layers and to inject holes efficiently into emitters in LEDs or reduce potential loss at the interface of hole extraction from the photoactive layer in SCs, (2) high mechanical, chemical and electrical stability, (3) good film-forming property enough to smooth the rough surface of the electrode and (4) high transmittance for efficient light extraction in LEDs and light absorption in SCs.

Although conventional anode buffer layers, such as small organic molecules and transition metal oxides have good hole injection or extraction properties, they are not suitable for solution processes or flexible optoelectronic applications. Conducting polymers can fulfill the requirements for solution processes and flexible devices. Conducting polymers, which have high versatility in molecular design and processing, constitute the most promising candidate for efficient anode buffer layer.

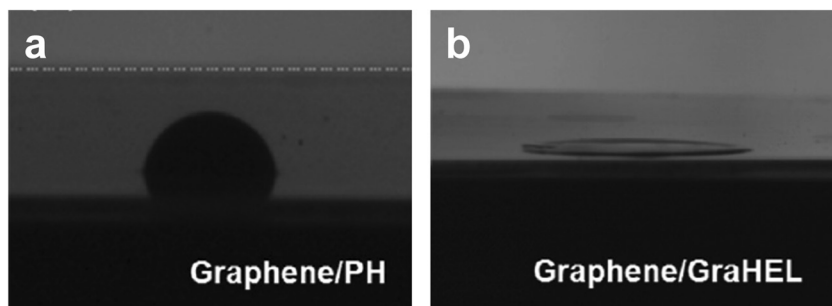


Figure 16. Contact angles of a) PEDOT:PSS and b) PEDOT:PSS:PFI on top of graphene. a,b) Reproduced with permission.^[271] Copyright 2016, WILEY-VCH.

Table 2. Summary of characteristics of SCs with different conducting polymer-based anode buffer layers.

Anode/conducting polymer-based anode buffer layers	Device Architecture	$V_{oc}^{a)}$ [V]	$J_{sc}^{b)}$ [mA cm ⁻²]	FF ^{c)} [%]	PCE ^{d)} [%]	Device degradation rate ^{e)}	Ref.
ITO/PEDOT:PSS	CH ₃ NH ₃ PbI ₃ /C ₆₀ /Bphen/Ag	0.97	16.11	63	9.81	≈10 d/20%	[43]
ITO/MoO ₃ /PEDOT:PSS		0.96	20.06	67	12.78	10d/93%	
ITO/PEDOT:PSS	TQ1:PC ₇₀ BM/LiF/Al	0.90	9.2	66	5.5	10 d/0%	[45]
ITO/PEDOT:PSS:MoO ₃		0.89	10.3	70	6.4	10 d/80%	
ITO/PEDOT:PSS	CH ₃ NH ₃ PbI _{3-x} Cl _x /PCBM/Bphen/Ag	0.92	20.91	72.61	13.90		[44]
ITO/PEDOT:PSS:MoO ₃		0.97	21.59	75.42	15.79		
ITO/PEDOT:PSS	CH ₃ NH ₃ PbI ₃ /PCBM/LiF/Ag	0.80	14.35	71.61	8.23	≈300 h/0%	[45]
ITO/GO/PEDOT:PSS		0.84	15.72	73.71	9.74	≈500 h/20%	
ITO/PEDOT:PSS	PTB7:PC ₇₀ BM/Al	0.75	14.75	63.6	7.04		[246]
ITO/PEDOT:PSS:GO		0.76	16.42	65.8	8.21		
ITO/PEDOT:PSS	CH ₃ NH ₃ PbI ₃ /PCBM/Al	0.835	14.1	68.5	8.1		[37]
ITO/PEDOT:PSS:PFI		0.982	16.7	70.5	11.7		
ITO/PEDOT:PSS	PCDTBT:PC ₇₀ BM	0.738	10.2	56.4	4.2		[38]
ITO/PEDOT:PSS:PFI		0.880	11.9	59.7	6.3		
ITO/PEDOT:PSS	CH ₃ NH ₃ PbI ₃ /PCBM/Al	0.903 ± 0.06	13.15 ± 64	62.8 ± 5.34	7.08 ± 1.88		
ITO/PEDOT:PSS:PFI		1.022 ± 0.023	15.29 ± 1.26	70.9 ± 3.41	10.90 ± 0.77		
ITO/PEDOT:PSS	PTB7-Th:PC ₇₁ BM	0.80	14.31	64.20	7.35		[270]
ITO/PEDOT:PSS:PFI		0.80	22.10	55.51	9.82		
ITO/PEDOT:PSS	CH ₃ NH ₃ PbI ₃ /PCBM/Al	0.923	11.8	73	7.8	186 h/50%	[39]
ITO/PSS-g-PANI		1.04	14.1	67.3	9.7	267 h/50%	
ITO/PSS-g-PANI:PFI		1.07	14.9	77.6	12.4	570 h/50%	
Graphene/PEDOT:PSS:PFI	P3HT:PC ₆₀ BM/Ca/Al	0.546	8.67	59.7	2.83		[271]
	PCDTBT:PC ₆₀ BM/Ca/Al	0.896	8.83	54.7	4.33		

^{a)} V_{oc} : open-circuit voltage; ^{b)} J_{sc} : short-circuit current; ^{c)}FF: fill factor; ^{d)}PCE: power conversion efficiency. ^{e)}Device degradation rate: device operation time until the PCE maintained certain percentage of its initial PCE.

The most widely-used conducting polymer anode buffer layer is PEDOT:PSS; and recently, its use has extended to OIHP optoelectronics. However, PEDOT:PSS is hygroscopic and highly acidic; these traits often cause severe degradation of the devices. Also, in most systems, the WF of PEDOT:PSS (5.0–5.2 eV for Clevios™ P VP AI4083) is too low to facilitate charge injection or to maintain high V_{oc} , because organic materials have deep HOMO energy level ≈5.5 eV and OIHP materials have deep VBM of 5.4–6.0 eV.

Therefore, several material engineering technologies have been used to overcome the demerits of PEDOT:PSS, while improving its advantages. These technologies include modifying material composition or molecular structure of conducting polymers. To reduce the hygroscopic and acidic properties of PEDOT:PSS film, which originated from the sulfonic acid groups of the PSS chains, the surface concentration of the PSS in the film has been controlled by using polar solvent to remove some free PSS at the surface. Also, several studies have introduced additives such as NaOH, guanidine, and imidazole to the aqueous PEDOT:PSS to reduce the water absorption and acidity of PEDOT:PSS, and consequently to increase the device stability. To reduce the water-sensitivity of buffer layers based on conducting polymers, the use of organo-soluble and non-corrosive conducting polymer has been suggested as an alternative

to the hygroscopic and acidic PEDOT:PSS. Recently, conducting polymer-based composite buffer layer with inorganic materials (e.g., MoO₃, GO) have been used to improve the stability of the conventional conducting polymer. Water-dispersible conducting polymers are unstable due to particle aggregation induced by de-doping during storage and device operation. Therefore, water-soluble self-doped conducting polymer (e.g. PSS-g-PANI) which has excellent stability and film-forming properties can be an alternative to PEDOT:PSS.

Conducting polymer-based composite or polymer blend anode buffer layers (e.g., PEDOT:PSS:MoO₃, PEDOT:PSS:GO, PEDOT:PSS:PFI) have been introduced. Anode buffer layers based on these composite increased charge transport in the device, and thus increased its efficiency and stability. Especially, PFI, which has low surface energy and high ionization potential, developed gradually increasing WF as a result of self-organization of polymer chains, and effectively increased the surface WF of both PEDOT:PSS and PSS-g-PANI. When the conducting polymer composites with inorganic materials such as MoO₃ and GO, and conducting polymer blends with PFI were used as anode buffer layers in LEDs, both efficiency and lifetime were greatly increased. This improvement was attributed to well-aligned energy level without large energy barrier between the buffer layer and the overlying semiconducting

layer, and facilitated hole injection; furthermore, the enrichment of insulating PFI molecules at the surface effectively block electrons and excitons reducing non-radiative recombination.

In SCs, the addition of a small amount of PFI to the conducting polymer also increased PCE and lifetime regardless of the photoactive materials used. The increased surface WF of conducting polymer blends by adding PFI was confirmed by the increase in V_{OC} . The improved PCE has been attributed to the increased V_{bi} in device. Also, the enrichment of PFI at the surface blocks diffusion of impurities into the photoactive layers and prolongs the lifetime of SCs as well.

Conducting polymer-based anode buffer layers have strong advantages because of their adjustable properties and high processability. For organic and OIHP optoelectronics to advance, efforts to develop stable and efficient anode buffer layers should continue. Conducting polymers have been dispersed or dissolved in water, but desirable development of future conducting polymers is soluble in organic solvents which can allow device fabrication in N_2 atmosphere; influences of oxygen and moisture in ambient condition that degrade device stability can be effectively eliminated. Cross-linking of conducting polymers also can be one of the effective solutions for further improvement in film stability of conducting polymer based anode buffer layers. The cross-linked conducting polymer-based anode buffer materials can be achieved by synthesizing polymers containing cross-linkable groups or adding cross-linking agents. Additionally, further investigation should seek multi-functional anode buffer layers that can provide device simplification of organic and OIHP optoelectronic devices.^[5,31]

Acknowledgements

S.A., S.-H.J. and T.-H.H. contributed equally to this work. This research was supported by the Nano Material Technology Development Program through the National Research Foundation of Korea (NRF) funded by the Ministry of Science, ICT & Future Planning (MSIP, Korea) (NRF-2014M3A7B4051747) and by the Agency for Defense Development (UD140044GD), Republic of Korea.

Received: July 1, 2016

Revised: August 29, 2016

Published online: November 9, 2016

- [1] A. J. Mäkinen, I. G. Hill, R. Shashidhar, N. Nikolov, Z. H. Kafafi, *Appl. Phys. Lett.* **2001**, *79*, 557.
- [2] S. A. Choulis, V.-E. Choong, M. K. Mathai, F. So, *Appl. Phys. Lett.* **2005**, *87*, 113503.
- [3] T.-W. Lee, Y. Chung, *Adv. Funct. Mater.* **2008**, *18*, 2246.
- [4] T.-W. Lee, Y. Chung, O. Kwon, J.-J. Park, *Adv. Funct. Mater.* **2007**, *17*, 390.
- [5] T.-H. Han, M.-R. Choi, S.-H. Woo, S.-Y. Min, C.-L. Lee, T.-W. Lee, *Adv. Mater.* **2012**, *24*, 1487.
- [6] T.-H. Han, Y. Lee, M.-R. Choi, S.-H. Woo, S.-H. Bae, B. H. Hong, J.-H. Ahn, T.-W. Lee, *Nat. Photonics* **2012**, *6*, 105.
- [7] A. Benor, S. Takizawa, C. Pérez-Bolívar, J. Pavel Anzenbacher, *Org. Electron.* **2010**, *11*, 938.
- [8] T.-H. Han, W. Song, T.-W. Lee, *ACS Appl. Mater. Interfaces* **2015**, *7*, 3117.
- [9] M.-R. Choi, T.-H. Han, K.-G. Lim, S.-H. Woo, D. H. Huh, T.-W. Lee, *Angew. Chem. Int. Ed.* **2011**, *50*, 6274.
- [10] K.-G. Lim, M.-R. Choi, J.-H. Kim, D. H. Kim, G. H. Jung, Y. Park, J.-L. Lee, T.-W. Lee, *ChemSusChem* **2014**, *7*, 1125.
- [11] Y. H. Kim, C. Sachse, M. L. MacHala, C. May, L. Müller-Meskamp, K. Leo, *Adv. Funct. Mater.* **2011**, *21*, 1076.
- [12] S.-I. Na, S.-S. Kim, J. Jo, D.-Y. Kim, *Adv. Mater.* **2008**, *20*, 4061.
- [13] J. W. Jung, J. U. Lee, W. H. Jo, *J. Phys. Chem. C* **2010**, *114*, 633.
- [14] M.-R. Choi, S.-H. Woo, T.-H. Han, K.-G. Lim, S.-Y. Min, W. M. Yun, O. K. Kwon, C. E. Park, K.-D. Kim, H.-K. Shin, M.-S. Kim, T. Noh, J. H. Park, K.-H. Shin, J. Jang, T.-W. Lee, *ChemSusChem* **2011**, *4*, 363.
- [15] A. R. bin Mohd Yusoff, D. Kim, H. P. Kim, F. K. Shneider, W. J. da Silva, J. Jang, *Energy Environ. Sci.* **2015**, *8*, 303.
- [16] H. Sirringhaus, T. Kawase, R. H. Friend, T. Shimoda, M. Inbasekaran, W. Wu, E. P. Woo, *Science* **2000**, *290*, 2123.
- [17] N. Stutzmann, R. H. Friend, H. Sirringhaus, *Science* **2003**, *299*, 1881.
- [18] K. Hong, S. Y. Yang, C. Yang, S. H. Kim, D. Choi, C. E. Park, *Org. Electron.* **2008**, *9*, 864.
- [19] D. Nilsson, T. Kugler, P. O. Svensson, M. Berggren, *Sensors Actuators, B* **2002**, *86*, 193.
- [20] L. Basicicò, P. Cosseddu, A. Scidà, B. Fraboni, G. G. Malliaras, A. Bonfigli, *Org. Electron.* **2012**, *13*, 244.
- [21] M. H. Bolin, K. Svennersten, D. Nilsson, A. Sawatdee, E. W. H. Jager, A. Richter-Dahlfors, M. Berggren, *Adv. Mater.* **2009**, *21*, 4379.
- [22] D. Khodagholy, J. Rivnay, M. Sessolo, M. Gurfinkel, P. Leleux, L. H. Jimison, E. Stavrinidou, T. Herve, S. Sanaur, R. M. Owens, G. G. Malliaras, *Nat. Commun.* **2013**, *4*, 2133.
- [23] J. Qi, L. Ni, D. Yang, X. Zhou, W. Qiao, M. Li, D. Ma, Z. Y. Wang, *J. Mater. Chem. C* **2014**, *2*, 2431.
- [24] Y. Yao, Y. Liang, V. Shrotriya, S. Xiao, L. Yu, Y. Yang, *Adv. Mater.* **2007**, *19*, 3979.
- [25] X. Gong, M. Tong, Y. Xia, W. Cai, J. S. Moon, Y. Cao, G. Yu, C.-L. Shieh, B. Nilsson, A. J. Heeger, *Science* **2009**, *325*, 1665.
- [26] B. Friedel, P. E. Keivanidis, T. J. K. Brenner, A. Abrusci, C. R. McNeill, R. H. Friend, N. C. Greenham, *Macromolecules* **2009**, *42*, 6741.
- [27] X. Gong, M. H. Tong, S. H. Park, M. Liu, A. Jen, A. J. Heeger, *Sensors* **2010**, *10*, 6488.
- [28] Z. Liu, K. Parvez, R. Li, R. Dong, X. Feng, K. Müllen, *Adv. Mater.* **2015**, *27*, 669.
- [29] Z.-K. Tan, R. S. Moghaddam, M. L. Lai, P. Docampo, R. Higler, F. Deschler, M. Price, A. Sadhanala, L. M. Pazos, D. Credginton, F. Hanusch, T. Bein, H. J. Snaith, R. H. Friend, *Nat. Nanotechnol.* **2014**, *9*, 687.
- [30] Y.-H. Kim, H. Cho, J. H. Heo, T.-S. S. Kim, N. Myoung, C.-L. Lee, S. H. Im, T.-W. Lee, *Adv. Mater.* **2015**, *27*, 1248.
- [31] H. Cho, S.-H. Jeong, M.-H. Park, Y.-H. Kim, C. Wolf, C.-L. Lee, J. H. Heo, A. Sadhanala, N. Myoung, S. Yoo, S. H. Im, R. H. Friend, T.-W. Lee, *Science* **2015**, *350*, 1222.
- [32] J. C. Yu, D. Bin Kim, E. D. Jung, B. R. Lee, M. H. Song, *Nanoscale* **2016**, *8*, 7036.
- [33] G. Li, Z. K. Tan, D. Di, M. L. Lai, L. Jiang, J. H. W. Lim, R. H. Friend, N. C. Greenham, *Nano Lett.* **2015**, *15*, 2640.
- [34] Y. Ling, Z. Yuan, Y. Tian, X. Wang, J. C. Wang, Y. Xin, K. Hanson, B. Ma, H. Gao, *Adv. Mater.* **2016**, *28*, 305.
- [35] N. K. Kumawat, A. Dey, K. L. Narasimhan, D. Kabra, *ACS Photonics* **2015**, *2*, 349.
- [36] X. Zhang, H. Lin, H. Huang, C. Reckmeier, Y. Zhang, W. C. H. Choy, A. L. Rogach, *Nano Lett.* **2016**, *16*, 1415.
- [37] K.-G. Lim, H.-B. Kim, J. Jeong, H. Kim, J. Y. Kim, T.-W. Lee, *Adv. Mater.* **2014**, *26*, 6461.
- [38] K.-G. Lim, S. Ahn, Y.-H. Kim, Y. Qi, T.-W. Lee, *Energy Environ. Sci.* **2016**, *9*, 932.

- [39] K.-G. Lim, S. Ahn, H. Kim, M.-R. Choi, D. H. Huh, T.-W. Lee, *Adv. Mater. Interfaces* **2016**, *3*, 1500678.
- [40] H. Kim, K.-G. Lim, T.-W. Lee, *Energy Environ. Sci.* **2016**, *9*, 12.
- [41] J. H. Heo, H. J. Han, D. Kim, T. K. Ahn, S. H. Im, *Energy Environ. Sci.* **2015**, *8*, 1602.
- [42] Z.-K. Wang, M. Li, D.-X. Yuan, X.-B. Shi, H. Ma, L.-S. Liao, *ACS Appl. Mater. Interfaces* **2015**, *7*, 9645.
- [43] F. Hou, Z. Su, F. Jin, X. Yan, L. Wang, H. Zhao, J. Zhu, B. Chu, W. Li, *Nanoscale* **2015**, *7*, 9427.
- [44] Y. Jiang, C. Li, H. Liu, R. Qin, H. Ma, *J. Mater. Chem. A* **2016**, *4*, 9958.
- [45] D.-Y. Lee, S.-I. Na, S.-S. Kim, *Nanoscale* **2016**, *8*, 1513.
- [46] M. Qian, M. Li, X.-B. Shi, H. Ma, Z.-K. Wang, L.-S. Liao, *J. Mater. Chem. A* **2015**, *3*, 13533.
- [47] A. Kahn, N. Koch, W. Gao, *J. Polym. Sci. Part B Polym. Phys.* **2003**, *41*, 2529.
- [48] S. A. Choulis, V. E. Choong, A. Patwardhan, M. K. Mathai, F. So, *Adv. Funct. Mater.* **2006**, *16*, 1075.
- [49] M. Graetzel, R. A. J. Janssen, D. B. Mitzi, E. H. Sargent, *Nature* **2012**, *488*, 304.
- [50] M. Taleb, G. Teyssède, S. Le Roy, C. Laurent, *IEEE Trans. Dielectr. Electr. Insul.* **2013**, *20*, 311.
- [51] K.-B. Kim, Y.-H. Tak, Y.-S. Han, K.-H. Baik, M.-H. Yoon, M.-H. Lee, *Jpn. J. Appl. Phys.* **2003**, *42*, L438.
- [52] Y.-H. Tak, K.-B. Kim, H.-G. Park, K.-H. Lee, J.-R. Lee, *Thin Solid Films* **2002**, *411*, 12.
- [53] F. Z. Dahou, L. Cattin, J. Garnier, J. Ouerfelli, M. Morsli, G. Louarn, A. Bouteville, A. Khellil, J. C. Bernède, *Thin Solid Films* **2010**, *518*, 6117.
- [54] G. Sakamoto, C. Adachi, T. Koyama, Y. Taniguchi, C. D. Merritt, H. Murata, Z. H. Kafafi, *Appl. Phys. Lett.* **1999**, *75*, 766.
- [55] J. Y. Shen, X. L. Yang, T. H. Huang, J. T. Lin, T. H. Ke, L. Y. Chen, C. C. Wu, M. C. P. Yeh, *Adv. Funct. Mater.* **2007**, *17*, 983.
- [56] K. Okumoto, H. Kanno, Y. Hamaa, H. Takahashi, K. Shibata, *Appl. Phys. Lett.* **2006**, *89*, 063504.
- [57] H. Nakanotani, T. Higuchi, T. Furukawa, K. Masui, K. Morimoto, M. Numata, H. Tanaka, Y. Sagara, T. Yasuda, C. Adachi, *Nat. Commun.* **2014**, *5*, 4016.
- [58] T. Furukawa, H. Nakanotani, M. Inoue, C. Adachi, *Sci. Rep.* **2015**, *5*, 8429.
- [59] X. Yan, B. Chu, W. Li, Z. Su, T. Zhang, F. Jin, B. Zhao, F. Zhang, D. Fan, Y. Gao, T. Tsuboi, J. Wang, H. Pi, J. Zhu, *Org. Electron.* **2013**, *14*, 1805.
- [60] S. L. M. Van Mensfoort, V. Shabro, R. J. De Vries, R. A. J. Janssen, R. Coehoorn, *J. Appl. Phys.* **2010**, *107*, 113710.
- [61] X. Zhou, J. Blochwitz, M. Pfeiffer, A. Nollau, T. Fritz, K. Leo, *Adv. Funct. Mater.* **2001**, *11*, 310.
- [62] A. Turak, *RSC Adv.* **2013**, *3*, 6188.
- [63] P. Fenter, F. Schreiber, V. Bulovi, S. R. Forrest, *Chem. Phys. Lett.* **1997**, *277*, 521.
- [64] X. Zhou, J. He, L. S. Liao, M. Lu, X. M. Ding, X. Y. Hou, X. M. Zhang, X. Q. He, S. T. Lee, *Adv. Mater.* **2000**, *12*, 265.
- [65] S. Tokito, H. Tanaka, K. Noda, A. Okada, Y. Taga, *IEEE Trans. Electron Devices* **1997**, *44*, 1239.
- [66] S. Yin, Z. Shuai, Y. Wang, *J. Chem. Inf. Comput. Sci.* **2003**, *43*, 970.
- [67] S. Tokito, H. Tanaka, K. Noda, A. Okada, Y. Taga, *Appl. Phys. Lett.* **1997**, *70*, 1929.
- [68] D. Grozea, A. Turak, Y. Yuan, S. Han, Z. H. Lu, W. Y. Kim, *J. Appl. Phys.* **2007**, *101*, 033522.
- [69] L. Sims, U. Hörmann, R. Hanfland, R. C. I. Mackenzie, F. R. Kogler, R. Steim, W. Brütting, P. Schilinsky, *Org. Electron.* **2014**, *15*, 2862.
- [70] J. Meyer, S. Hamwi, M. Kröger, W. Kowalsky, T. Riedl, A. Kahn, *Adv. Mater.* **2012**, *24*, 5408.
- [71] S. Tokito, K. Noda, Y. Taga, *J. Phys. D. Appl. Phys.* **1999**, *29*, 2750.
- [72] V. Shrotriya, G. Li, Y. Yao, C.-W. Chu, Y. Yang, *Appl. Phys. Lett.* **2006**, *88*, 073508.
- [73] J. Grosskreutz, *J. Electrochem. Soc.* **1969**, *116*, 1232.
- [74] F. Wang, Z. Tan, Y. Li, *Energy Environ. Sci.* **2015**, *8*, 1059.
- [75] L. "Bert" Groenendaal, F. Jonas, D. Freitag, H. Pielartzik, J. R. Reynolds, *Adv. Mater.* **2000**, *12*, 481.
- [76] S. H. Eom, S. Senthilarasu, P. Uthirakumar, S. C. Yoon, J. Lim, C. Lee, H. S. Lim, J. Lee, S. H. Lee, *Org. Electron.* **2009**, *10*, 536.
- [77] Q. Dong, Y. Zhou, J. Pei, Z. Liu, Y. Li, S. Yao, J. Zhang, W. Tian, *Org. Electron.* **2010**, *11*, 1327.
- [78] N. Kim, S. Kee, S. H. Lee, B. H. Lee, Y. H. Kahng, Y. R. Jo, B. J. Kim, K. Lee, *Adv. Mater.* **2014**, *26*, 2268.
- [79] F. Krebs, S. Gevorgyan, J. Alstrup, *J. Mater. Chem.* **2009**, *19*, 5442.
- [80] S. H. Eom, H. Park, S. H. Mujawar, S. C. Yoon, S. S. Kim, S. I. Na, S. J. Kang, D. Khim, D. Y. Kim, S. H. Lee, *Org. Electron.* **2010**, *11*, 1516.
- [81] C. K. Cho, W. J. Hwang, K. Eun, S. H. Choa, S. I. Na, H. K. Kim, *Sol. Energy Mater. Sol. Cells* **2011**, *95*, 3269.
- [82] T.-C. Li, R.-C. Chang, *Int. J. Precis. Eng. Manuf. Green Technol.* **2014**, *1*, 329.
- [83] J. McCarthy, C. Hanley, L. Brennan, V. Lambertini, Y. Gun'ko, *J. Mater. Chem. C* **2014**, *2*, 764.
- [84] Y. Chen, K. S. Kang, K. J. Han, K. H. Yoo, J. Kim, *Synth. Met.* **2009**, *159*, 1701.
- [85] B. Riedel, Y. Shen, J. Hauss, M. Aichholz, X. Tang, U. Lemmer, M. Gerken, *Adv. Mater.* **2011**, *23*, 740.
- [86] Y. Xu, Y. Wang, J. Liang, Y. Huang, Y. Ma, X. Wan, Y. Chen, *Nano Res.* **2009**, *2*, 343.
- [87] U. Lang, J. Dual, *Key Eng. Mater.* **2007**, *345-346*, 1189.
- [88] U. Lang, N. Naujoks, J. Dual, *Synth. Met.* **2009**, *159*, 473.
- [89] L. Jin, T. Wang, Z.-Q. Feng, M. K. Leach, J. Wu, S. Mo, Q. Jiang, *J. Mater. Chem. B* **2013**, *1*, 1818.
- [90] M. P. de Jong, L. J. van Ijzendoorn, M. J. a. de Voigt, *Appl. Phys. Lett.* **2000**, *77*, 2255.
- [91] V. Singh, S. Arora, M. Arora, V. Sharma, R. P. Tandon, *Semicond. Sci. Technol.* **2014**, *29*, 045020.
- [92] S. Chen, L. Song, Z. Tao, X. Shao, Y. Huang, Q. Cui, X. Guo, *Org. Electron.* **2014**, *15*, 3654.
- [93] V. M. Drakonakis, A. Savva, M. Kokonou, S. A. Choulis, *Sol. Energy Mater. Sol. Cells* **2014**, *130*, 544.
- [94] T.-W. Lee, O. Kwon, M.-G. Kim, S. H. Park, J. Chung, S. Y. Kim, Y. Chung, J.-Y. Park, E. Han, D. H. Huh, J.-J. Park, L. Pu, *Appl. Phys. Lett.* **2005**, *87*, 231106.
- [95] J. Park, Y. Kwon, T.-W. Lee, *Macromol. Rapid Commun.* **2007**, *28*, 1366.
- [96] A. van Dijken, A. Perro, E. A. Meulenkaamp, K. Brunner, *Org. Electron.* **2003**, *4*, 131.
- [97] J. S. Kim, R. H. Friend, I. Grizzi, J. H. Burroughes, *Appl. Phys. Lett.* **2005**, *87*, 023506.
- [98] Y.-H. Kim, C. Wolf, H. Cho, S.-H. Jeong, T.-W. Lee, *Adv. Mater.* **2016**, *28*, 734.
- [99] H. Yan, P. Lee, N. R. Armstrong, A. Graham, G. A. Evmenenko, P. Dutta, T. J. Marks, *J. Am. Chem. Soc.* **2005**, *127*, 3172.
- [100] W. J. Bae, K. H. Kim, Y. H. Park, W. H. Jo, *Chem. Commun.* **2003**, 2768.
- [101] C. A. Cutler, M. Bouguettaya, T. S. Kang, J. R. Reynolds, *Macromolecules* **2005**, *38*, 3068.
- [102] R. H. Karlsson, A. Herland, M. Hamedi, J. A. Wigenius, A. Åslund, X. Liu, M. Fahlman, O. Ingana, P. Konradsson, *Chem. Mater.* **2009**, *21*, 1815.
- [103] W. R. Salaneck, R. H. Friend, J. L. Brédas, *Phys. Rep.* **1999**, *319*, 231.
- [104] R. E. Myers, *J. Electron. Mater.* **1986**, *15*, 61.

- [105] C. K. Chiang, C. R. Fincher, Y. W. Park, A. J. Heeger, H. Shirakawa, E. J. Louis, S. C. Gau, A. G. MacDiarmid, *Phys. Rev. Lett.* **1977**, *39*, 1098.
- [106] A. J. Heeger, *Polym. J.* **1985**, *17*, 201.
- [107] J. L. Bredas, G. B. G. Street, *Acc. Chem. Res.* **1985**, *18*, 309.
- [108] N. Massonnet, A. Carella, A. de Geyer, J. Faure-Vincent, J.-P. Simonato, *Chem. Sci.* **2015**, *6*, 412.
- [109] S. Etemad, A. J. Heeger, *Annu. Rev. Phys. Chem.* **1982**, *33*, 443.
- [110] A. J. Heeger, S. Kivelson, J. R. Schrieffer, W.-P. Su, *Rev. Mod. Phys.* **1988**, *60*, 781.
- [111] M. Kertesz, Y. S. Lee, *J. Phys. Chem.* **1987**, 2690.
- [112] D. D. C. Bradley, *J. Phys. D. Appl. Phys.* **1987**, *20*, 1389.
- [113] W. R. Salaneck, N. Sato, R. Lazzaroni, M. Lögdglund, *Vacuum* **1990**, *41*, 1648.
- [114] R. R. Chance, D. S. Boudreaux, J. L. Bredas, R. Silbey, in *Handbook of Conducting Polymers*, Marcel Dekker, New York **1986**, p. 825.
- [115] J. L. Brbdas, R. Silbey, D. S. Boudreaux, R. R. Chance, *J. Am. Chem. Soc.* **1983**, *105*, 6555.
- [116] K. K. Kanazawa, A. F. Diaz, R. H. Geiss, W. D. Gill, J. F. Kwak, J. A. Logan, J. F. Rabolt, G. B. Street, *J. Chem. Soc. Chem. Commun.* **1979**, 854.
- [117] W.-S. Huang, B. D. Humphrey, A. G. MacDiarmid, *J. Chem. Soc. Faraday Trans. 1* **1986**, *82*, 2385.
- [118] J. C. Chiang, A. G. MacDiarmid, *Synth. Met.* **1986**, *13*, 193.
- [119] R. Corradi, S. P. Armes, *Synth. Met.* **1997**, *84*, 453.
- [120] A. G. MacDiarmid, *Angew. Chem. Int. Ed.* **2001**, *40*, 2581.
- [121] J. Z. Wang, J. F. Chang, H. Siringhaus, *Appl. Phys. Lett.* **2005**, *87*, 083503.
- [122] C. K. Chiang, Y. W. Park, A. J. Heeger, H. Shirakawa, E. J. Louis, A. G. MacDiarmid, *J. Chem. Phys.* **1978**, *69*, 5098.
- [123] H. Shirakawa, E. J. Louis, A. G. MacDiarmid, C. K. Chiang, A. J. Heeger, *J. Chem. Soc. Chem. Commun.* **1977**, 578.
- [124] T. T. Osamu Niwa, *J. Chem. Soc., Chem. Commun.* **1984**, 817.
- [125] P. M. McManus, S. C. Yang, R. J. Cushman, *J. Chem. Soc. Chem. Commun.* **1985**, 1556.
- [126] F. Genoud, M. Guglielmi, M. Nechtschein, E. Genies, M. Salmon, *Phys. Rev. Lett.* **1985**, *55*, 118.
- [127] J. Joo, J. Lee, J. Baeck, K. Kim, E. Oh, J. Epstein, *Synth. Met.* **2001**, *117*, 45.
- [128] Y. Shen, M. Wan, *Synth. Met.* **1998**, *96*, 127.
- [129] T. E. Olinga, J. Fraysse, J. P. Travers, A. Dufresne, A. Pron, *Macromolecules* **2000**, *33*, 2107.
- [130] F. Louwet, L. Groenendaal, J. Dhaen, J. Manca, J. Van Luppen, E. Verdonck, L. Leenders, *Synth. Met.* **2003**, *135-136*, 115.
- [131] J. E. Yoo, J. L. Cross, T. L. Bucholz, K. S. Lee, M. P. Espe, Y.-L. Loo, *J. Mater. Chem.* **2007**, *17*, 1268.
- [132] N. Gospodinova, L. Terlemezyan, *Prog. Polym. Sci.* **1998**, *23*, 1443.
- [133] N. Gospodinova, L. Terlemezyan, P. Mokreva, K. Kossev, *Polymer* **1993**, *34*, 2434.
- [134] J. P. Lock, S. G. Im, K. K. Gleason, *Macromolecules* **2006**, *39*, 5326.
- [135] S. G. Im, K. K. Gleason, *Macromolecules* **2007**, *40*, 6552.
- [136] J. Storsberg, H. Ritter, H. Pielartzik, L. Groenendaal, *Adv. Mater.* **2000**, *12*, 567.
- [137] I. Sapurina, J. Stejskal, *Polym. Int.* **2008**, *57*, 1295.
- [138] H. Li, G. Shi, W. Ye, C. Li, Y. Liang, *J. Appl. Polym. Sci.* **1997**, *64*, 2149.
- [139] G. Zotti, S. Zecchin, G. Schiavon, F. Louwet, L. Groenendaal, X. Crispin, W. Osikowicz, W. Salaneck, M. Fahlman, *Macromolecules* **2003**, *36*, 3337.
- [140] S. Sinha, S. Bhadra, D. Khastgir, *J. Appl. Polym. Sci.* **2009**, *112*, 3135.
- [141] H. Moon, J. Park, *J. Polym. Sci. Part A Polym. Chem.* **1998**, *36*, 1431.
- [142] D. Kumar, R. C. Sharma, *Eur. Polym. J.* **1998**, *34*, 1053.
- [143] S.-A. Chen, L.-C. Lin, *Macromolecules* **1995**, *28*, 1239.
- [144] H. J. Snaith, H. Kenrick, M. Chiesa, R. H. Friend, *Polymer* **2005**, *46*, 2573.
- [145] R. W. T. Higgins, N. A. Zaidi, A. P. Monkman, *Adv. Funct. Mater.* **2001**, *11*, 407.
- [146] O. Abdulrazzaq, S. E. Bourdo, V. Saini, F. Watanabe, B. Barnes, A. Ghosh, A. S. Biris, *RSC Adv.* **2015**, *5*, 33.
- [147] J. Gao, A. J. Heeger, J. Y. Lee, C. Y. Kim, *Synth. Met.* **1996**, *82*, 221.
- [148] P. D. Gaikwad, D. J. Shirale, V. K. Gade, P. A. Savale, K. P. Kakde, H. J. Kharat, M. D. Shirsat, *Bull. Mater. Sci.* **2006**, *29*, 417.
- [149] A. C. Roy, V. S. Nisha, C. Dhand, M. A. Ali, B. D. Malhotra, *Anal. Chim. Acta* **2013**, *777*, 63.
- [150] G. Sonmez, P. Schottland, J. R. Reynolds, *Synth. Met.* **2005**, *155*, 130.
- [151] N. V. Konoshchuk, O. Y. Posudievsky, O. L. Gribkova, A. A. Nekrasov, A. V. Vannikov, V. H. Koshechko, V. D. Pokhodenko, *Theor. Exp. Chem.* **2014**, *50*, 21.
- [152] Y. Wang, J. Zhang, D. Sheng, C. Sun, *J. Chromatogr. A* **2010**, *1217*, 4523.
- [153] L. Xu, Z. Chen, W. Chen, A. Mulchandani, Y. Yan, *Macromol. Rapid Commun.* **2008**, *29*, 832.
- [154] K. R. Choudhury, J. Lee, N. Chopra, A. Gupta, X. Jiang, F. Amy, F. So, *Adv. Funct. Mater.* **2009**, *19*, 491.
- [155] J. Huang, P. F. Miller, J. S. Wilson, A. J. De Mello, J. C. De Mello, D. D. C. Bradley, *Adv. Funct. Mater.* **2005**, *15*, 290.
- [156] J. H. Burroughes, D. D. C. Bradley, A. R. Brown, R. N. Marks, K. Mackay, R. H. Friend, P. L. Burns, A. B. Holmes, *Nature* **1990**, *347*, 539.
- [157] N. C. Greenham, S. C. Moratti, D. D. C. Bradley, R. H. Friend, A. B. Holmes, *Nature* **1993**, *365*, 628.
- [158] T.-W. Lee, H.-C. Lee, O. O. Park, *Appl. Phys. Lett.* **2002**, *81*, 214.
- [159] Y. Yang, A. J. Heeger, *Appl. Phys. Lett.* **1994**, *64*, 1245.
- [160] S. Karg, J. C. Scott, J. R. Salem, M. Angdopoulos, *Synth. Met.* **1996**, *80*, 111.
- [161] J. Jang, J. Ha, K. Kim, *Thin Solid Films* **2008**, *516*, 3152.
- [162] H. A. Ahmad, D. Nayak, S. Panda, *J. Appl. Polym. Sci.* **2013**, *129*, 230.
- [163] T. Stöcker, A. Köhler, R. Moos, *J. Polym. B: Polym. Phys.* **2012**, *50*, 976.
- [164] C.-C. Chen, W.-H. Chang, K. Yoshimura, K. Ohya, J. You, J. Gao, Z. Hong, Y. Yang, *Adv. Mater.* **2014**, *26*, 5670.
- [165] O. Abdulrazzaq, S. E. Bourdo, M. Woo, V. Saini, B. C. Berry, A. Ghosh, A. S. Biris, *ACS Appl. Mater. Interfaces* **2015**, *7*, 27667.
- [166] Y. R. Park, H. J. Kim, S. Im, S. Seo, K. Shin, W. K. Choi, Y. J. Hong, *Appl. Phys. Lett.* **2016**, *108*, 023301.
- [167] T. J. Marks, J. G. C. Veinot, J. Cui, H. Yan, A. Wang, N. L. Edleman, J. Ni, Q. Huang, P. Lee, N. R. Armstrong, *Synth. Met.* **2002**, *127*, 29.
- [168] J. Cui, A. Wang, N. L. Edleman, J. Ni, P. Lee, N. R. Armstrong, T. J. Marks, *Adv. Mater.* **2001**, *13*, 1476.
- [169] J.-H. Bae, J.-M. Moon, S. W. Jeong, J.-J. Kim, J.-W. Kang, D.-G. Kim, J.-K. Kim, J.-W. Park, H.-K. Kim, *J. Electrochem. Soc.* **2008**, *155*, J1.
- [170] K. H. Choi, H. J. Nam, J. A. Jeong, S. W. Cho, H. K. Kim, J. W. Kang, D. G. Kim, W. J. Cho, *Appl. Phys. Lett.* **2008**, *92*, 223302.
- [171] S.-J. Yoo, H.-J. Yun, I. Kang, K. Thangaraju, S.-K. Kwon, Y.-H. Kim, *J. Mater. Chem. C* **2013**, *1*, 2217.
- [172] B. S. Kim, J. Y. Lee, *Adv. Funct. Mater.* **2014**, *24*, 3970.
- [173] C. Soci, I. W. Hwang, D. Moses, Z. Zhu, D. Waller, R. Gaudiana, C. J. Brabec, A. J. Heeger, *Adv. Funct. Mater.* **2007**, *17*, 632.
- [174] C. Liu, C. Yi, K. Wang, Y. Yang, R. S. Bhatta, M. Tsigie, S. Xiao, X. Gong, *ACS Appl. Mater. Interfaces* **2015**, *7*, 4928.
- [175] E. Zhou, J. Cong, K. Hashimoto, K. Tajima, *Adv. Mater.* **2013**, *25*, 6991.
- [176] H.-L. Yip, A. K.-Y. Jen, *Energy Environ. Sci.* **2012**, *5*, 5994.

- [177] T.-W. Lee, T. Noh, H.-W. Shin, O. Kwon, J.-J. Park, B.-K. Choi, M.-S. Kim, D. W. Shin, Y.-R. Kim, *Adv. Funct. Mater.* **2009**, *19*, 1625.
- [178] J. J. Park, T. J. Park, W. S. Jeon, R. Pode, J. Jang, J. H. Kwon, E.-S. Yu, M.-Y. Chae, *Org. Electron.* **2009**, *10*, 189.
- [179] L. Duan, L. Hou, T.-W. Lee, J. Qiao, D. Zhang, G. Dong, L. Wang, Y. Qiu, *J. Mater. Chem.* **2010**, *20*, 6392.
- [180] J. Chen, C. Shi, Q. Fu, F. Zhao, Y. Hu, Y. Feng, D. Ma, *J. Mater. Chem.* **2012**, *22*, 5164.
- [181] M. D. Irwin, D. B. Buchholz, A. W. Hains, R. P. H. Chang, T. J. Marks, *Proc. Natl. Acad. Sci. USA* **2008**, *105*, 2783.
- [182] A. Bulusu, S. A. Paniagua, B. A. Macleod, A. K. Sigdel, J. J. Berry, D. C. Olson, S. R. Marder, S. Graham, *Langmuir* **2013**, *29*, 3935.
- [183] J. R. Manders, S. Tsang, M. J. Hartel, T. Lai, S. Chen, C. M. Amb, J. R. Reynolds, F. So, *Adv. Funct. Mater.* **2013**, *23*, 2993.
- [184] C. P. Chen, Y. D. Chen, S. C. Chuang, *Adv. Mater.* **2011**, *23*, 3859.
- [185] A. R. Schlattmann, D. W. Floet, A. Hilberer, F. Garten, P. J. M. Smulders, T. M. Klapwijk, G. Hadziioannou, *Appl. Phys. Lett.* **1996**, *69*, 1764.
- [186] Z. Chen, *Thin Solid Films* **2001**, *394*, 202.
- [187] B. R. Lee, J. J. Y. Kim, D. Kang, D. W. Lee, S.-J. Ko, H. J. Lee, C.-L. Lee, H. S. Shin, M. H. Song, *ACS Nano* **2012**, *6*, 2984.
- [188] J. Liu, Y. Xue, Y. Gao, D. Yu, M. Durstock, L. Dai, *Adv. Mater.* **2012**, *24*, 2228.
- [189] E. Stratakis, K. Savva, D. Konios, C. Petridis, E. Kymakis, *Nanoscale* **2014**, *6*, 6925.
- [190] X. Liu, H. Kim, L. J. Guo, *Org. Electron.* **2013**, *14*, 591.
- [191] S.-S. Li, K.-H. Tu, C.-C. Lin, C.-W. Chen, M. Chhowalla, *ACS Nano* **2010**, *4*, 3169.
- [192] G. Venugopal, K. Krishnamoorthy, R. Mohan, S.-J. Kim, *Mater. Chem. Phys.* **2012**, *132*, 29.
- [193] K. Krishnamoorthy, M. Veerapandian, K. Yun, S. J. Kim, *Carbon* **2013**, *53*, 38.
- [194] E. Vitoratos, S. Sakkopoulos, N. Paliatsas, K. Emmanouil, S. A. Choulis, *Open J. Org. Polym. Mater.* **2012**, *2*, 7.
- [195] E. Mosconi, J. M. Azpiroz, F. De Angelis, *Chem. Mater.* **2015**, *27*, 4885.
- [196] A. Guerrero, J. You, C. Aranda, Y. S. Kang, G. Garcia-Belmonte, H. Zhou, J. Bisquert, Y. Yang, *ACS Nano* **2016**, *10*, 218.
- [197] T. A. Berhe, W.-N. Su, C.-H. Chen, C.-J. Pan, J.-H. Cheng, H.-M. Chen, M.-C. Tsai, L.-Y. Chen, A. A. Dubale, B.-J. Hwang, *Energy Environ. Sci.* **2016**, *9*, 323.
- [198] Y. Jiao, F. Ma, G. Gao, H. Wang, J. Bell, T. Frauenheim, A. Du, *RSC Adv.* **2015**, *5*, 82346.
- [199] J. Yang, B. D. Siempelkamp, D. Liu, T. L. Kelly, *ACS Nano* **2015**, *9*, 1955.
- [200] J. A. Christians, P. A. Miranda Herrera, P. V. Kamat, *J. Am. Chem. Soc.* **2015**, *137*, 1530.
- [201] C.-J. Tong, W. Geng, Z.-K. Tang, C.-Y. Yam, X.-L. Fan, J. Liu, W.-M. Lau, L.-M. Liu, *J. Phys. Chem. Lett.* **2015**, *6*, 3289.
- [202] X. Dong, X. Fang, M. Lv, B. Lin, S. Zhang, J. Ding, N. Yuan, *J. Mater. Chem. A* **2015**, *3*, 5360.
- [203] J. Zhao, B. Cai, Z. Luo, Y. Dong, Y. Zhang, H. Xu, B. Hong, Y. Yang, L. Li, W. Zhang, C. Gao, *Sci. Rep.* **2016**, *6*, 21976.
- [204] M. Shirayama, M. Kato, T. Miyadera, T. Sugita, T. Fujiseki, S. Hara, H. Kadowaki, D. Murata, M. Chikamatsu, H. Fujiwara, *J. Appl. Phys.* **2016**, *119*, 115501.
- [205] H. G. Jeon, Y. H. Huh, S. H. Yun, K. W. Kim, S. S. Lee, J. Lim, K.-S. An, B. Park, *J. Mater. Chem. C* **2014**, *2*, 2622.
- [206] I. D. Parker, *J. Appl. Phys.* **1994**, *75*, 1656.
- [207] N. K. Elumalai, A. Uddin, *Energy Environ. Sci.* **2016**, *9*, 391.
- [208] M. R. Lenze, N. M. Kronenberg, F. Würthner, K. Meerholz, *Org. Electron.* **2015**, *21*, 171.
- [209] P.-J. Chia, L.-L. Chua, S. Sivaramakrishnan, J.-M. Zhuo, L.-H. Zhao, W.-S. Sim, Y.-C. Yeo, P. K.-H. Ho, *Adv. Mater.* **2007**, *19*, 4202.
- [210] M. M. de Kok, M. Buechel, S. I. E. Vulto, P. van de Weijer, E. A. Meulenkaamp, S. H. P. M. de Winter, A. J. G. Mank, H. J. M. Vorstenbosch, C. H. L. Weijtens, V. van Elsbergen, *Phys. status solidi* **2004**, *201*, 1342.
- [211] O. P. Dimitriev, Y. P. Piryatinski, A. A. Pud, *J. Phys. Chem. B* **2011**, *115*, 1357.
- [212] H. J. Snaith, H. Kenrick, M. Chiesa, R. H. Friend, *Polymer* **2005**, *46*, 2573.
- [213] T. L. Kelly, Y. Yamada, S. P. Y. Che, K. Yano, M. O. Wolf, *Adv. Mater.* **2008**, *20*, 2616.
- [214] Y. Xia, J. Ouyang, *J. Mater. Chem.* **2011**, *21*, 4927.
- [215] H. Yan, H. Okuzaki, *Synth. Met.* **2009**, *159*, 2225.
- [216] B. Friedel, T. J. K. Brenner, C. R. McNeill, U. Steiner, N. C. Greenham, *Org. Electron.* **2011**, *12*, 1736.
- [217] P. C. Jukes, S. J. Martin, A. M. Higgins, M. Geoghegan, R. A. L. Jones, S. Langridge, A. Wehrum, S. Kirchmeyer, *Adv. Mater.* **2004**, *16*, 807.
- [218] J.-S. Yeo, J.-M. Yun, D.-Y. Kim, S. Park, S.-S. Kim, M.-H. Yoon, T.-W. Kim, S.-I. Na, *ACS Appl. Mater. Interfaces* **2012**, *4*, 2551.
- [219] J. Huang, P. F. Miller, J. C. De Mello, A. J. De Mello, D. D. C. Bradley, *Synth. Met.* **2003**, *139*, 569.
- [220] D. A. Mengistie, P.-C. Wang, C.-W. Chu, *J. Mater. Chem. A* **2013**, *1*, 9907.
- [221] J. Rivnay, S. Inal, B. A. Collins, M. Sessolo, E. Stavrinidou, X. Strakosas, C. Tassone, D. M. Delongchamp, G. G. Malliaras, *Nat. Commun.* **2016**, *7*, 11287.
- [222] S. Savagatrup, E. Chan, S. M. Renteria-Garcia, A. D. Printz, A. V. Zaretski, T. F. O'Connor, D. Rodriguez, E. Valle, D. J. Lipomi, *Adv. Funct. Mater.* **2015**, *25*, 427.
- [223] J. Ouyang, Q. Xu, C. W. Chu, Y. Yang, G. Li, J. Shinar, *Polymer* **2004**, *45*, 8443.
- [224] D. Alemu, H.-Y. Wei, K.-C. Ho, C.-W. Chu, *Energy Environ. Sci.* **2012**, *5*, 9662.
- [225] J. Y. Kim, J. H. Jung, D. E. Lee, J. Joo, *Synth. Met.* **2002**, *126*, 311.
- [226] X. Crispin, F. L. E. Jakobsson, A. Crispin, P. C. M. Grim, P. Andersson, A. Volodin, C. van Haesendonck, M. Van der Auweraer, W. R. Salaneck, M. Berggren, *Chem. Mater.* **2006**, *18*, 4354.
- [227] J. Ouyang, C. W. Chu, F. C. Chen, Q. Xu, Y. Yang, *Adv. Funct. Mater.* **2005**, *15*, 203.
- [228] T.-C. Tsai, H.-C. Chang, C.-H. Chen, Y.-C. Huang, W.-T. Whang, *Org. Electron.* **2014**, *15*, 641.
- [229] Y. Meng, Z. Hu, N. Ai, Z. Jiang, J. Wang, J. Peng, Y. Cao, *ACS Appl. Mater. Interfaces* **2014**, *6*, 5122.
- [230] H. Kim, S. Nam, H. Lee, S. Woo, C. S. Ha, M. Ree, Y. Kim, *J. Phys. Chem. C* **2011**, *115*, 13502.
- [231] S. Kim, S. Y. Kim, M. H. Chung, J. Kim, J. H. Kim, *J. Mater. Chem. C* **2015**, *3*, 5859.
- [232] R. Wang, S. Chen, L. Feng, Q. Li, W. Hu, W. Liu, X. Guo, *Org. Electron.* **2015**, *27*, 259.
- [233] A. Cho, S. Kim, S. Kim, W. Cho, C. Park, F. S. Kim, J. H. Kim, *J. Polym. Sci. Part B Polym. Phys.* **2016**, *54*, 1530.
- [234] T. Kim, M. Suh, S. J. Kwon, T. H. Lee, J. E. Kim, Y. J. Lee, J. H. Kim, P. M. Hong, K. S. Suh, *Macromol. Rapid Commun.* **2009**, *30*, 1477.
- [235] J. Liu, L. N. Lewis, A. R. Duggal, *Appl. Phys. Lett.* **2007**, *90*, 233503.
- [236] H. Zhang, Q. Fu, W. Zeng, D. Ma, *J. Mater. Chem. C* **2014**, *2*, 9620.
- [237] S. Shao, J. Liu, J. Bergqvist, S. Shi, C. Veit, U. Würfel, Z. Xie, F. Zhang, *Adv. Energy Mater.* **2013**, *3*, 349.
- [238] Y. Wang, Q. Luo, N. Wu, Q. Wang, H. Zhu, L. Chen, Y. Q. Li, L. Luo, C. Q. Ma, *ACS Appl. Mater. Interfaces* **2015**, *7*, 7170.
- [239] Q. Liu, I. Khatri, R. Ishikawa, K. Ueno, H. Shirai, *Appl. Phys. Lett.* **2013**, *102*, 183503.
- [240] H. S. Dehsari, E. K. Shalamzari, J. N. Gavvani, F. A. Taromi, S. Ghanbary, *RSC Adv.* **2014**, *4*, 55067.

- [241] M. Ono, Z. Tang, R. Ishikawa, T. Gotou, K. Ueno, H. Shirai, *Appl. Phys. Express* **2012**, 5, 032301.
- [242] J.-H. Lin, J.-J. Zeng, Y.-C. Su, Y.-J. Lin, *Appl. Phys. Lett.* **2012**, 100, 153509.
- [243] Y.-J. Lin, F.-M. Yang, C.-Y. Huang, W.-Y. Chou, J. Chang, Y.-C. Lien, *Appl. Phys. Lett.* **2007**, 91, 092127.
- [244] J. Hwang, F. Amy, A. Kahn, *Org. Electron.* **2006**, 7, 387.
- [245] M. Petrosino, A. Rubino, *Synth. Met.* **2012**, 161, 271.
- [246] J. C. Yu, J. I. Jang, B. R. Lee, G. Lee, J. T. Han, M. H. Song, *ACS Appl. Mater. Interfaces* **2014**, 6, 2067.
- [247] J. Lee, H. Kang, S. Kee, S. H. Lee, S. Y. Jeong, G. Kim, J. Kim, S. Hong, H. Back, K. Lee, *ACS Appl. Mater. Interfaces* **2016**, 8, 6144.
- [248] C. W. Tang, S. A. Vanslyke, *Appl. Phys. Lett.* **1987**, 51, 913.
- [249] S. D. Stranks, G. E. Eperon, G. Grancini, C. Menelaou, M. J. P. Alcocer, T. Leijtens, L. M. Herz, A. Petrozza, H. J. Snaith, *Science* **2013**, 342, 341.
- [250] A. Kojima, K. Teshima, Y. Shirai, T. Miyasaka, *J. Am. Chem. Soc.* **2009**, 131, 6050.
- [251] S. R. Forrest, D. D. C. Bradley, M. E. Thompson, *Adv. Mater.* **2003**, 15, 1043.
- [252] M. A. Baldo, D. F. O'Brien, M. E. Thompson, S. R. Forrest, *Phys. Rev. B* **1999**, 60, 14422.
- [253] B. A. Köhler, J. S. Wilson, R. H. Friend, *Adv. Eng. Mater.* **2002**, 4, 453.
- [254] M. A. Baldo, M. E. Thompson, S. R. Forrest, *Pure Appl. Chem.* **1999**, 71, 2095.
- [255] M. A. Baldo, M. E. Thompson, S. R. Forrest, *Nature* **2000**, 403, 750.
- [256] P. D. Fleischauer, P. Fleischauer, *Chem. Rev.* **1970**, 70, 199.
- [257] H. Uoyama, K. Goushi, K. Shizu, H. Nomura, C. Adachi, *Nature* **2012**, 492, 234.
- [258] Y. Tang, J. Zhuang, L. Xie, X. Chen, D. Zhang, J. Hao, W. Su, Z. Cui, *Eur. J. Org. Chem.* **2016**, 3737.
- [259] J. K. Park, G. S. Hwang, B. D. Chin, N. S. Kang, T.-W. Lee, *Curr. Appl. Phys.* **2012**, 12, 38.
- [260] K. S. Novoselov, A. K. Geim, S. V. Morozov, D. Jiang, Y. Zhang, S. V. Dubonos, I. V. Grigorieva, A. A. Firsov, *Science* **2004**, 306, 666.
- [261] Y. B. Zhang, Y. W. Tan, H. L. Stormer, P. Kim, *Nature* **2005**, 438, 201.
- [262] K. S. Kim, Y. Zhao, H. Jang, S. Y. Lee, J. M. Kim, K. S. Kim, J.-H. Ahn, P. Kim, J.-Y. Choi, B. H. Hong, *Nature* **2009**, 457, 706.
- [263] S. Bae, H. Kim, Y. Lee, X. Xu, J.-S. Park, Y. Zheng, J. Balakrishnan, T. Lei, H. Ri Kim, Y. Il Song, Y.-J. Kim, K. S. Kim, B. Özyilmaz, J.-H. Ahn, B. H. Hong, S. Iijima, *Nat. Nanotechnol.* **2010**, 5, 574.
- [264] G. Xing, N. Mathews, S. S. Lim, Y. M. Lam, S. Mhaisalkar, T. C. Sum, *Science* **2013**, 342, 344.
- [265] Q. Dong, Y. Fang, Y. Shao, P. Mulligan, J. Qiu, L. Cao, J. Huang, *Science* **2015**, 347, 967.
- [266] G. Li, R. Zhu, Y. Yang, *Nat. Photonics* **2012**, 6, 153.
- [267] D. J. Lipomi, H. Chong, M. Vosgueritchian, J. Mei, Z. Bao, *Sol. Energy Mater. Sol. Cells* **2012**, 107, 355.
- [268] D. J. Lipomi, B. C. K. Tee, M. Vosgueritchian, Z. Bao, *Adv. Mater.* **2011**, 23, 1771.
- [269] A. Polman, M. Knight, E. C. Garnett, B. Ehrler, W. C. Sinke, *Science* **2016**, 352, 6283.
- [270] L. Zhao, S. Zhao, Z. Xu, D. Huang, J. Zhao, Y. Li, X. Xu, *ACS Appl. Mater. Interfaces* **2016**, 8, 547.
- [271] H. Kim, S. Bae, T.-H. Han, K.-G. Lim, J.-H. Ahn, T.-W. Lee, *Nanotechnology* **2014**, 25, 014012.
- [272] X. Bulliard, S.-G. Ihn, S. Yun, Y. Kim, D. Choi, J.-Y. Choi, M. Kim, M. Sim, J.-H. Park, W. Choi, K. Cho, *Adv. Funct. Mater.* **2010**, 20, 4381.
- [273] C. Bi, Q. Wang, Y. Shao, Y. Yuan, Z. Xiao, J. Huang, *Nat. Commun.* **2015**, 6, 7747.
- [274] W. J. da Silva, A. R. bin Mohd Yusoff, J. Jang, *IEEE Electron Device Lett.* **2013**, 34, 1566.